TR 226

Technical Report 226

ENERGY BALANCE ON A PAVED SURFACE

Richard L. Berg

June 1974

PREPARED FOR
DIRECTORATE OF MILITARY CONSTRUCTION
OFFICE, CHIEF OF ENGINEERS
BY

CORPS OF ENGINEERS, U.S. ARMY
COLD REGIONS RESEARCH AND ENGINEERING LABORATORY
HANOVER, NEW HAMPSHIRE

The findings in this report are not to be construed as an official Department of the Army position unless so designated by other authorized documents.

ENERGY BALANCE ON A PAVED SURFACE

Richard L. Berg

June 1974

PREPARED FOR
DIRECTORATE OF MILITARY CONSTRUCTION
OFFICE, CHIEF OF ENGINEERS
BY

CORPS OF ENGINEERS, U.S. ARMY
COLD REGIONS RESEARCH AND ENGINEERING LABORATORY
HANOVER, NEW HAMPSHIRE

PREFACE

Authority for the investigation reported herein is contained in FY 1965 Instructions and Outline, Military Construction Investigations, Engineering Criteria and Investigations and Studies, Investigation of Arctic Construction; Sub-project 42, Thermal Calculation Techniques.

The Military Construction Investigations program is conducted for the Directorate of Military Construction, Office of the Chief of Engineers. This investigation was under the technical direction of the Engineering Division of this directorate, Advanced Technology Branch, Civil Engineering Section (F.B. Hennion, Chief).

This report was prepared by R.L. Berg, Research Civil Engineer, of the Northern Engineering Research Branch (W.F. Quinn, Chief), Experimental Engineering Division (K.A. Linell, Chief), U.S. Army Cold Regions Research and Engineering Laboratory (USA CRREL).

The micrometeorological data were measured, reduced and tabulated by a U.S. Army Meteorological Support Team commanded by Master Sergeant Paul D. Lamb, NCOIC. The team was assigned to USA CRREL by the U.S. Army Electronics Command Meteorological Support Activity.

This report was technically reviewed by W.F. Quinn and E.F. Lobacz of USA CRREL.

The contents of this report are not to be used for advertising, publication, or promotional purposes. Citation of trade names does not constitute an official endorsement of approval of the use of such commercial products.

CONTENTS

ILLUSTRATIONS

CONTENTS (Cont'd)

ILLUSTRATIONS (Cont'd)

TABLES

SYMBOLS

Symbol	*Meaning*	*Units*
A	Surface albedo	Dimensionless
B	Bowen ratio	Dimensionless
C_a	Average daily cloud cover	10ths
C_d	Average cloud cover during daylight hours	10ths
H_s	Heat of sublimation of snow	Btu/lb
K	Atmospheric transmission coefficient	Dimensionless
P_L	Clear-day longwave radiation	%
P_s	Clear-day shortwave radiation	%
Q_a	Heat flux by net all-wave radiation	Btu/sq ft day
Q_{abs}	Heat flux by absorbed shortwave radiation	Btu/sq ft day
Q_c	Heat flux by convection	Btu/sq ft day
Q_e	Heat flux by terrestrial longwave radiation	Btu/sq ft day
Q_g	Heat flux by conduction into the ground	Btu/sq ft day
Q_{g1}	Heat flux into ground, example 1	Btu/sq ft
Q_{g2}	Heat flux into ground, example 2	Btu/sq ft
Q_i	Heat flux by infiltration of moisture	Btu/sq ft day
Q_l	Heat flux by evaporation, condensation and sublimation	Btu/sq ft day
Q_m	Heat flux by precipitation	Btu/sq ft day
Q_n	Heat flux by net longwave radiation	Btu/sq ft day
Q_r	Heat flux by reflected shortwave radiation	Btu/sq ft day
Q_s	Heat flux by incident shortwave radiation	Btu/sq ft day
Q_u	Heat flux by conduction into the air	Btu/sq ft day
Q_w	Heat flux by atmospheric longwave radiation	Btu/sq ft day
R	Correlation coefficient	Dimensionless
S	Standard error	%
T_a	Air temperature	°F, °R
T_s	Surface temperature	°F, °R
X_1	Frost depth, example 1	ft
X_2	Frost depth, example 2	ft
Z_1	Height above surface, sensor 1	ft
Z_2	Height above surface, sensor 2	ft

SYMBOLS (Cont'd)

Symbol	*Meaning*	*Units*
a	Regression coefficient, constant	-
b	Regression coefficient, constant	-
c	Regression coefficient, constant	-
c_p	Specific heat at constant pressure	Btu/lb °F
d	Regression coefficient, constant	-
f	Empirical constant	-
h	Heat transfer coefficient	Btu/sq ft day °F
k	von Karman's constant	Dimensionless
n	Sample size	Dimensionless
t	Time, Julian day number	day
u	Wind velocity	mph
v	Vapor pressure	mm of Hg
x	Value of independent variable	-
y	Value of dependent variable	-
ΔQ	Difference in heat flux	%
ΔT	Temperature difference	°F
ΔX	Difference in frost depth	%
Δs	Thickness of snow layer	ft
Δu	Difference in wind speed	ft/day
θ	Phase angle	radians
ϵ_a	Emissivity of atmosphere	Dimensionless
ϵ_s	Emissivity of pavement surface	Dimensionless
ρ	Density of air	lb/cu ft
ρ_s	Density of snow	lb/cu ft
σ	Stefan-Boltzmann constant	Btu/sq ft day °R

ENERGY BALANCE ON A PAVED SURFACE

by

Richard L. Berg

INTRODUCTION

Information obtained from two test sections paved with portland cement concrete, located at the Lebanon Regional Airport, Lebanon, New Hampshire, is analyzed in this report. The test slabs were constructed for two reasons: (1) to determine the effectiveness of an insulating material in reducing frost penetration beneath a pavement, and (2) to evaluate and refine techniques currently used by the Departments of the Army and the Air Force (1965; 1966a, b) for calculating frost and thaw penetration depths and subsurface temperatures.

This report primarily concerns the computational accuracy of individual energy balance components and total energy balance at the surface of the test slabs.

Techniques for computing frost or thaw depths are briefly reviewed to illustrate applications of the surface energy balance in frost and thaw depth calculations.

Micrometeorological data were obtained during the 1963-1964, 1964-1965, 1965-1966 and 1966-1967 winters. Because data from the 1963-1964 winter are not complete, comparisons between measured and calculated data are made for the last three winters only. Initial data were acquired on an earlier date each succeeding year. Inclusive dates are:

8 Dec 1964 - 31 Mar 1965
17 Nov 1965 - 31 Mar 1966
20 Oct 1966 - 31 Mar 1967.

SITE DESCRIPTION

The test slabs are located at the Lebanon Regional Airport, Lebanon, New Hampshire. This airport is 2.5 miles west of Lebanon and about 1 mile east of the Connecticut River, at 43°30' north latitude and 72°19' west longitude. It is on a plateau at an elevation of 562 ft (mean sea level) and is surrounded by hills with peak elevations of 1000 ft to 1350 ft. Figure 1 gives an aerial view of the test area and Figure 2 shows plan and profile views of the test slabs.

Meteorological data, from information obtained by the Federal Aviation Administration (FAA), are given in Table I. The FAA station is approximately ¼ mile west of the test site.

Table I. Meteorological data, 1943-1968.*

Air temperature (°F)		*Total precipitation (in.)*	
Mean annual (23 years record)	48.9	Mean annual (22 years record)	35.8
Recorded high (18 June 1957)	99	Maximum annual (1954)	43.5
Recorded low (14 Jan 1957)	–34	Maximum monthly (Aug 1955)	9.0
Air freezing index (°days F)		*Snowfall (in.)*	
Mean (1944-1966)	1170	Mean annual (22 years record)	76
Design (1947)	1777	Maximum annual (1958)	102
1963-1964	1461	Average duration of freeze days	120
1964-1965	1330	Average duration of thaw days	245
1965-1966	1204		
1966-1967	1405		

*Data obtained by FAA station (U.S. Department of Commerce, 1963-1967a) at Lebanon Regional Airport, about ¼ mile from test site.

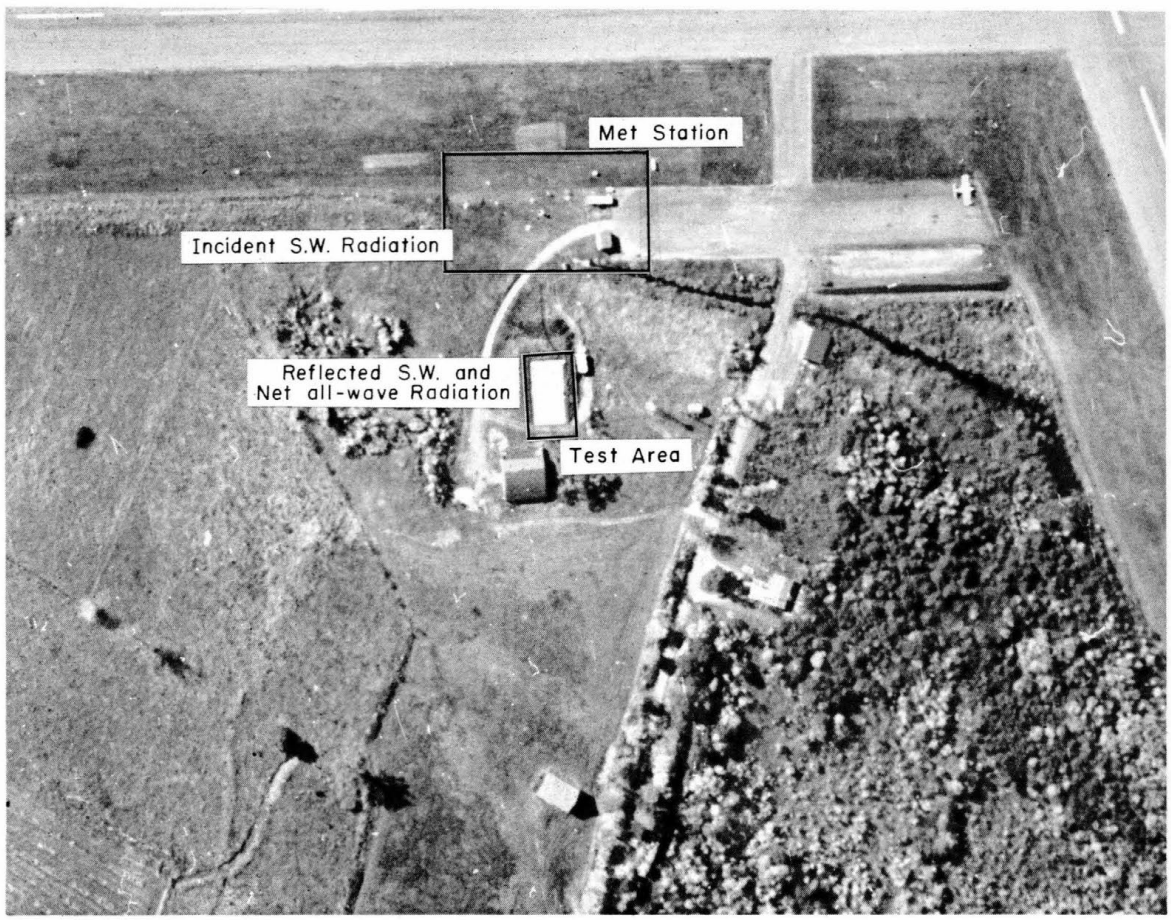

Figure 1. Aerial view of test area.

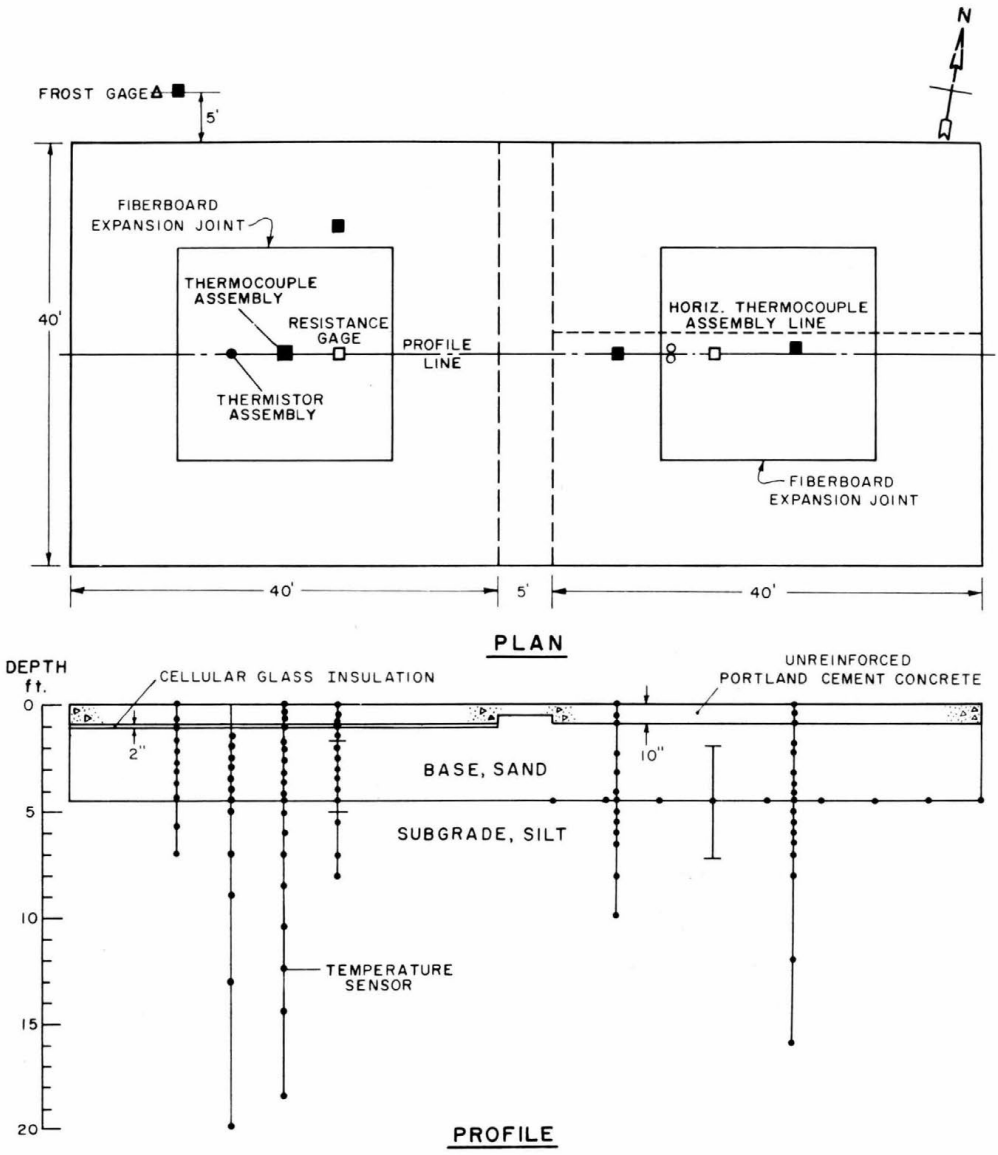

Figure 2. Plan and profile views of test slabs.

INSTRUMENTATION

Micrometeorological parameters were measured only during the winters but subsurface temperatures were observed throughout the year. Micrometeorological parameters measured are listed in Table II. Subsurface instrumentation is shown in Figure 2 and surface instrumentation is shown in Figure 3. All parameters listed in Table II were recorded continuously during the winters by the U.S. Army Meteorological Support Team assigned to the U.S. Army Cold Regions Research and Engineering Laboratory (USA CRREL). Recorders were recalibrated biweekly and sensors were recalibrated prior to installation each season.

Incident and reflected solar radiation were measured with 50-junction Eppley pyrheliometers responsive to wavelengths shorter than 3.5 μ. The manufacturer states that probable error for the

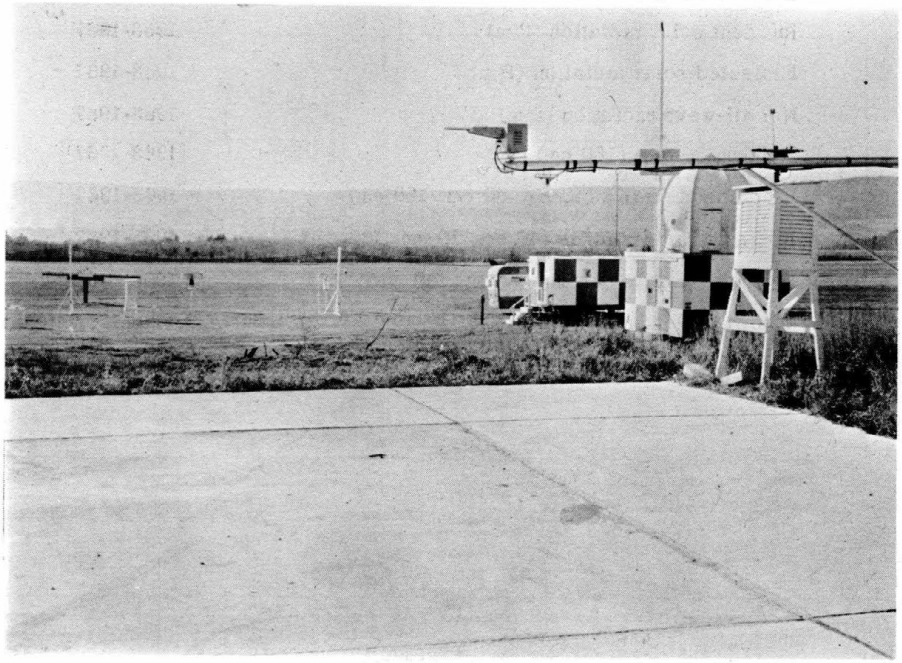

a. *Radiometers and instrument shelter.*

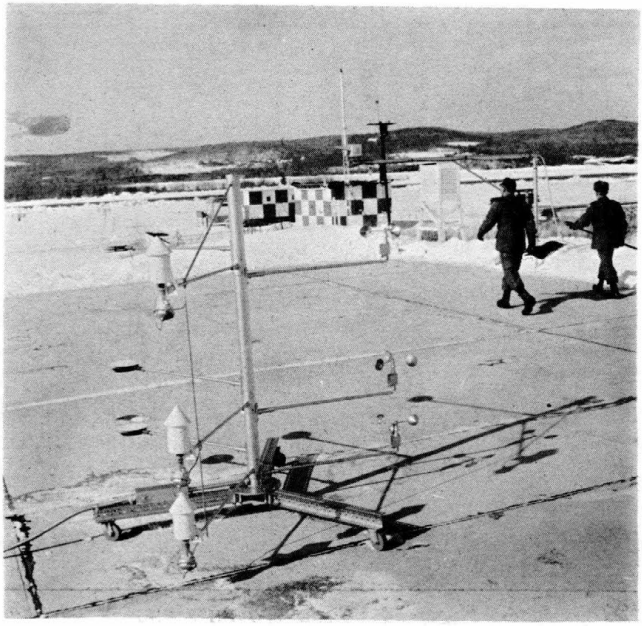

b. *Mast with dew cells, anemometers and air temperature thermocouples.*

Figure 3. Micrometeorological equipment at test site.

Table II. Micrometeorological parameters measured.

Parameters	*Period*
Incident solar radiation (2 m)	1963-1967
Reflected solar radiation (2 m)	1963-1967
Net all-wave radiation (2 m)	1963-1967
Air temperature (160 cm)	1963-1967
Wind speed profile (40 cm, 80 cm, 160 cm)	1965-1967
Air temperature profile (40 cm, 80 cm, 160 cm)	1965-1967
Dewpoint profile (40 cm, 80 cm, 160 cm)	1965-1967
Total hemispherical radiation (2 m)	1965-1967

Figure 4. Snow around slabs.

instruments is about ±2%. A thorough discussion of the characteristics of these instruments is presented by Fuquay and Buettner (1957).

Net all-wave and total hemispherical radiation are measured with radiometers similar to those developed by Gier and Dunkle (1951). The manufacturers' stated accuracy of calibration is ±2% but Kondrat'yev (1965) indicated that the accuracy of measurements of net all-wave radiation is usually not greater than ±10%.

Data from air temperature profiles, wind speed profiles and dewpoint profiles were not used in this analysis for two reasons: 1) energy balance components are calculated by methods that do not require these data, and 2) additional turbulence is undoubtedly imparted to the air moving over the slabs due to abrupt discontinuities in snow depth around the perimeter of the slabs (Fig. 4). The nature of this added turbulence probably depends on wind speed, wind direction, and snow depth; therefore, trends computed using these data are not reliable.

FROST AND THAW DEPTHS

Three techniques for computing frost or thaw penetration depths are of primary concern in this project: 1) the modified Berggren equation developed by Aldrich and Paynter (1953) and currently used by the Departments of the Army and the Air Force (1966a), 2) Scott's cumulative heat flow technique (1959, 1963, 1969, 1970a, b); Massachusetts Institute of Technology (ACFEL, 1961), and 3) a finite difference technique discussed by Dusinberre (1961).

The modified Berggren equation is used by the Army and Air Force because it is relatively easily solved; it is generally accurate to within ±15% of the maximum observed frost or thaw depth (Aldrich and Paynter, 1953); and the only variables required for input are the surface index, length of the season, mean annual temperature and thermal properties of the soil layers. The first three variables have been studied in considerable detail and maps illustrating mean and design values are in Departments of the Army and the Air Force design manuals (1966b). Kersten (1949) presented information on thermal properties of soils.

Applying the cumulative heat flow technique is more complex than using the modified Berggren equation and requires additional input information. Data required for this technique are: average daily air temperature, average daily wind speed, daily radiation balance on the surface, average daily evaporation from the surface, mean annual temperature and thermal properties of the soil layers. Although this list does not appear significantly larger than that for the modified Berggren equation, additional variables, including average daily cloud cover, average cloud cover during daylight hours, type and height of clouds, relative humidity and average daily surface temperature, are required to compute quantities for the radiation balance, convection and evaporation.

Solution of heat flow problems using numerical techniques has become common with the widespread availability of electronic digital computers. Finite difference and finite element methods are readily adapted to input data similar to data for either the modified Berggren equation or the cumulative heat flow technique. Berg (1973) summarizes numerical methods that have been applied to heat flux in soils.

In the cumulative heat flow technique, the radiation balance, evaporative and convective losses are determined, transformed into an equivalent temperature and combined with air temperatures. The resulting temperature and a system function are used in numerical integration of the convolution integral to obtain cumulative heat flux through the surface and surface temperatures.

In this report, quantities of heat transferred to the surface by each component of the surface energy balance are calculated. Procedures used are similar to those proposed by Scott (1959, 1963, 1969, 1970a, b) and MIT (ACFEL, 1961).

ENERGY BALANCE TECHNIQUE

General equation

The energy balance at the air/ground interface is determined from:

$$0 = Q_s - Q_r + Q_w - Q_e \pm Q_c \pm Q_l \pm Q_u \pm Q_m \pm Q_g \pm Q_i . \quad (1)$$

Individual heat fluxes are due to:

Q_s = incident shortwave radiation

Q_r = reflected shortwave radiation

Q_w = longwave radiation emitted by the atmosphere

Q_e = longwave radiation emitted by the earth

Q_c = convection

Q_l = evaporation, condensation, sublimation, and evapotranspiration

Q_u = conduction into air

Q_m = mass flow to surface (precipitation)

Q_g = conduction into ground

Q_i = infiltration of moisture into ground.

Units are Btu/sq ft day. Components carrying heat toward the surface are positive, those carrying heat away from the surface are negative, and those that may flow in either direction are shown with both signs.

The thermal conductivity of air is very small so heat conduction into the air is generally neglected (Sellers, 1965). Portland cement concrete is essentially impervious to moisture so heat flux by infiltration is neglected in this study. Energy flux due to precipitation is also neglected.

Quantities of heat conducted into the ground are desired; therefore, eq 1 is rewritten neglecting fluxes due to conduction into the air, mass flow and infiltration:

$$Q_g = Q_s - Q_r + Q_w - Q_e \pm Q_c \pm Q_l . \quad (2)$$

Methods of calculating each component are discussed in the following sections.

Shortwave radiation

Shortwave radiation includes all radiative energy with wavelengths between 0.15 μ and 3.5 μ. It therefore includes direct and indirect solar radiation and back-scattered radiation from the atmosphere.

Several methods are available for calculating incident solar radiation under cloudless skies, but only those presented by Bolsenga (1964) and List (1963) are discussed here.

Bolsenga's (1964) information, determined by Klein's (1948) method, considers precipitable water content of the atmosphere, atmospheric dust attenuation, albedo of the earth and back-scattered radiation. Table III contains quantities of computed and measured incident solar radiation from Bolsenga (1964) for several cloudless days.

It is evident from these data that Bolsenga's technique generally provided quantities greater than measured ones. The average of the absolute values of individual differences is 12%. [Throughout this report individual differences are computed from: (Measured - calculated) × (100/measured) and averages of the absolute values of individual differences are used. Using an average based on absolute values eliminates the possibility of individual errors being large but compensated for.]

Scott (1969) computed incident solar radiation at Fairbanks, Alaska, from the Smithsonian Meteorological Tables (List, 1963), but his computed values are greater than the measured quantities. However, he used an atmospheric transmission coefficient of 0.9; and information from this study and others (Wilson, 1967; Byers, 1959) indicates that a more accurate approximation is 0.70 to 0.80. Applying a coefficient of 0.75 to Scott's data provides much better agreement with measured data (Fig. 5).

The average atmospheric transmission coefficient on clear days at the Lebanon Regional Airport, from Table III, is 0.71. The Smithsonian Meteorological Tables (List, 1963) and an atmospheric transmission coefficient of 0.71 are used to compute incident solar radiation at Lebanon, New Hampshire. Results in Table IV show very good agreement with data from Figure 6.

For areas at elevations greater than about 2000 ft, atmospheric transmission coefficients should be increased slightly, but Bolsenga (1964) indicated that quantities obtained with his technique differ from measured quantities by only about 10% at elevations up to 6300 ft. The results of Wilson (1967) and those in Table III indicate that transmission coefficients vary slightly from day to day, but a constant value was used in the equations in the following section.

Incident solar radiation on clear days is generally considered to vary sinusoidally, with a minimum value on the winter solstice, 21 December, and a maximum value on the summer solstice, 22 June (Wilson, 1967; Byers, 1959; Sellers, 1965a). The sinusoid has a period of one year, so it must pass through its mean value ¼ of its period, 91 days, after reaching its minimum value; the vernal equinox, 21 March, occurs at this time.

Appendix B and Figure 6 show quantities of incident solar radiation measured on clear days at Lebanon. Values for the 1963-1964 winter were greater than those for other years. Reasons for the differences may be due to miscalibration of the instrumentation or a decrease in the atmospheric transmission coefficient after the 1963-1964 winter. The former reason is more probable, but recalibration of the instrumentation was not possible when the differences were discovered. Data from the last three winters were more compatible and only these data were used to determine the most representative sine wave. The curve on Figure 6 reaches a minimum on 19 December rather than 21 December; therefore, it passes through its mean value on 19 March rather than on 21 March. Quantities of clear-day incident shortwave radiation on 19 December and 19 March are 660 Btu/sq ft day and 1780 Btu/sq ft day, respectively. The amplitude of the sine wave is simply the difference between incident shortwave radiational quantities on these days or 1120 Btu/sq ft day. The equations for the curve are:

Table III. Computed and measured incident solar radiation using Bolsenga's (1964) procedure.

Date	Dewpoint* temp (°F)	Albedo† (%)	Atmospheric** transmission coefficient	Solar radiation: Computed: Direct (Btu/sq ft day)	Computed: Backscattered (Btu/sq ft day)	Computed: Total (Btu/sq ft day)	Measured: Total (Btu/sq ft day)	Difference†† (%)
16 Dec 63	− 8	72	0.70	725	115	840	866	+ 3
15 Jan 64	− 9	77	.72	835	135	970	943	− 3
12 Feb 64	0	55	.73	1225	130	1355	1322	− 2
20 Mar 64	+16	65	.74	1670	205	1875	2143	+12
14 Nov 64	+24	35	.68	875	70	945	884	− 7
29 Dec 64	+10	77	.68	675	120	795	705	−13
21 Jan 65	+ 4	80	.71	835	145	980	869	− 9
17 Feb 65	+ 2	50	.73	1250	120	1370	1268	− 8
12 Mar 65	+ 6	35	.75	1585	105	1690	1646	− 3
26 Jun 65	+42	35	.62	2575	215	2790	2752	− 2
19 Oct 65	+48	35	.65	1185	95	1280	1070	−20
20 Dec 65	− 6	80	.71	755	115	870	705	−23
12 Jan 66	−15	80	.72	845	130	975	789	−24
8 Feb 66	− 4	77	.73	1125	160	1285	1142	−12
15 Mar 66	+11	77	.75	1670	225	1895	1778	− 7
15 Apr 66	+23	35	.74	2155	135	2290	2085	−10
21 Oct 66	+30	35	.70	1205	85	1290	1154	−12
13 Nov 66	+24	35	.70	1100	80	1180	900	−31
12 Dec 66	+14	35	.68	705	50	755	643	−18
18 Jan 67	−12	75	.72	910	130	1040	816	−28
12 Feb 67	−14	70	.74	1205	150	1355	1189	−14
19 Mar 67	+27	35	.73	1630	105	1735	1752	+ 1
			Avg 0.71					Avg*** 12

*Average of hourly observations during daylight.

†From measured values of incident and reflected solar radiation.

**From measured values incident at ground surface and theoretical values incident at top of atmosphere.

††(Measured-calculated) × (100/measured).

***Average of the absolute value of individual differences.

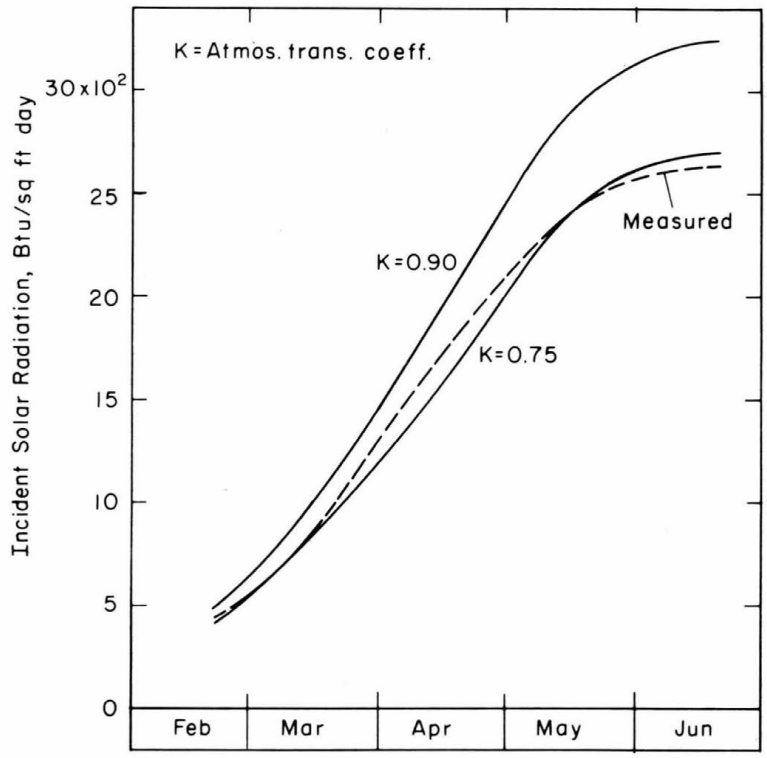

Figure 5. Incident solar radiation, Fairbanks, Alaska.

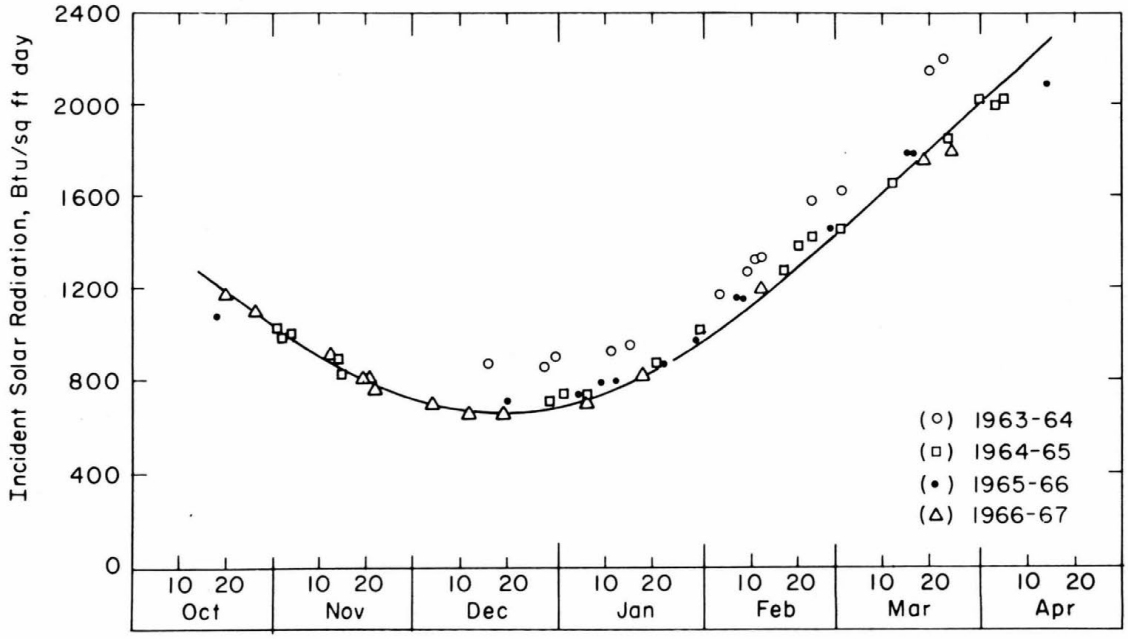

Figure 6. Measured incident solar radiation on clear days.

Table IV. Solar radiation on clear days.

Date	*Computed** *(Btu/sq ft day)*	*Measured†* *(Btu/sq ft day)*	*Difference*** *(%)*
8 Nov	985	985	0.0
30 Nov	785	760	–3.3
22 Dec	705	705	0.0
13 Jan	785	795	+1.3
4 Feb	995	1050	+5.2
26 Feb	1320	1270	–3.9
21 Mar	1690	1820	+7.1
			Avg†† 3.0

*Assumed atmospheric transmission coefficient of 0.71.
†From Figure 6.
**(Measured-calculated) × (100/measured).
††Average of absolute value of individual differences.

$$Q_s = 1780 + 1120 \sin \theta \tag{3}$$

$$\theta = 360/365\,(t - 78) \qquad t > 78 \tag{4}$$

$$\theta = 283 + 360t/365 \qquad t \leq 78 \tag{5}$$

t = Julian day number.

Since very few days are cloudless, a method of computing amounts of incident shortwave radiation on cloudy days is necessary. Several equations used in conjunction with clear-day quantities have been proposed (see Budyko, 1958; Department of the Interior, 1952; Dingman *et al.*, 1968; Geiger, 1965; Scott, 1959; Sellers, 1965a; Sutton, 1953). Nearly all of these equations determine the percentage of clear-day solar radiation and are functions of average cloud cover during daylight hours. To be more precise, parameters such as type, thickness, height and time of occurrence of clouds should also be considered; but data for these parameters are not usually available. The general form of equations relating percentage of possible clear-day incident shortwave radiation with cloud cover is polynomial:

$$P_s = a + bC_d + cC_d^2 + dC_d^3 \tag{6}$$

where

P_s = clear-day incident solar radiation, %

C_d = average cloud cover during daylight hours, 10ths

a, b, c, d, etc. = regression coefficients.

Polynomials ranging from fifth-order to linear were studied using 370 pairs of data from the three winters of this study. Examination of correlation coefficients and standard errors of each regression indicated that an equation of the form

$$P_s = a + cC_d^2 \tag{7}$$

provided results nearly as accurate as those of higher-order equations. Regression information obtained for eq 7 is $a = 96.00$, $c = -0.71$, correlation coefficient = 0.922 and standard error = 11.6. The correlation coefficient and standard error for a fifth-order polynomial are 0.928 and 11.2, respectively.

Equation 7 can be written as:

$$P_s = 96.00 - 0.71\, C_d^2 \tag{8}$$

which is similar to the equation Scott (1959) obtained from analysis of data from Thule, Greenland. His regression coefficients are $a = 100$ and $b = -0.67$.

In eq 8, clear-day incident solar radiation P_s does not equal 100% when $C_d = 0$ as it theoretically should. Regression data indicate $P_s = 96\%$ when $C_d = 0$, but this is not a serious error because only about 8% of the total days are clear days. A 4% difference on clear days is therefore a difference of less than 0.5% in monthly or seasonal totals of incident shortwave radiation. The 4% difference on clear days is also considerably less than the standard error of nearly 12%.

Figure 7 illustrates the effect of clouds on incident solar radiation. Since there are 370 points, only the range is shown for each value of average daily cloud cover. The curve from eq 8 is also shown.

Only the net quantity of shortwave radiation, i.e., that absorbed at the surface, influences the energy balance; the net quantity is the difference between incident and reflected quantities:

$$Q_{abs} = Q_s - Q_r \tag{9a}$$

$$= Q_s \left(1 - \frac{Q_r}{Q_s}\right) \tag{9b}$$

$$= Q_s (1 - A). \tag{9c}$$

A is defined as the surface albedo and can be measured or obtained from Table V, which is a collection of information from: American Society of Heating, Refrigerating and Air-Conditioning Engineers (ASHRAE) (1961), Sutton (1953), Wilson (1967), Budyko (1958), Byers (1959), Geiger (1965), List (1963) and Sellers (1965a).

Since daily totals of incident and reflected shortwave radiation were obtained from this test, the albedo was computed for each day. Figure 8 is a frequency histogram of albedoes determined for days when the slabs were dry; the mean albedo for these days was about 0.4. For days when rain or snow fell, albedoes were 0.5 and 0.7, respectively.

Monthly sums of absorbed shortwave radiation were obtained by summing daily totals determined by combining eq 3, 8 and 9c.

$$Q_{abs} = (1780 + 1120 \sin \theta)(1 - A)(0.96 - 0.0071\, C_d^2) \tag{10a}$$

$$= (1780 + 1120 \sin \theta)(0.6)(0.96 - 0.0071\, C_d^2). \tag{10b}$$

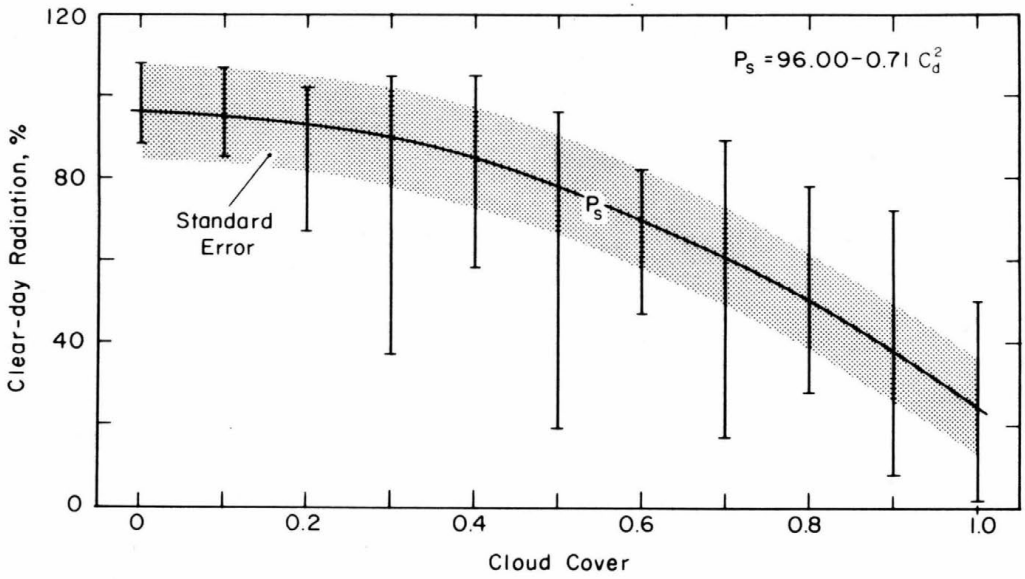

Figure 7. Effect of clouds on incident solar radiation.

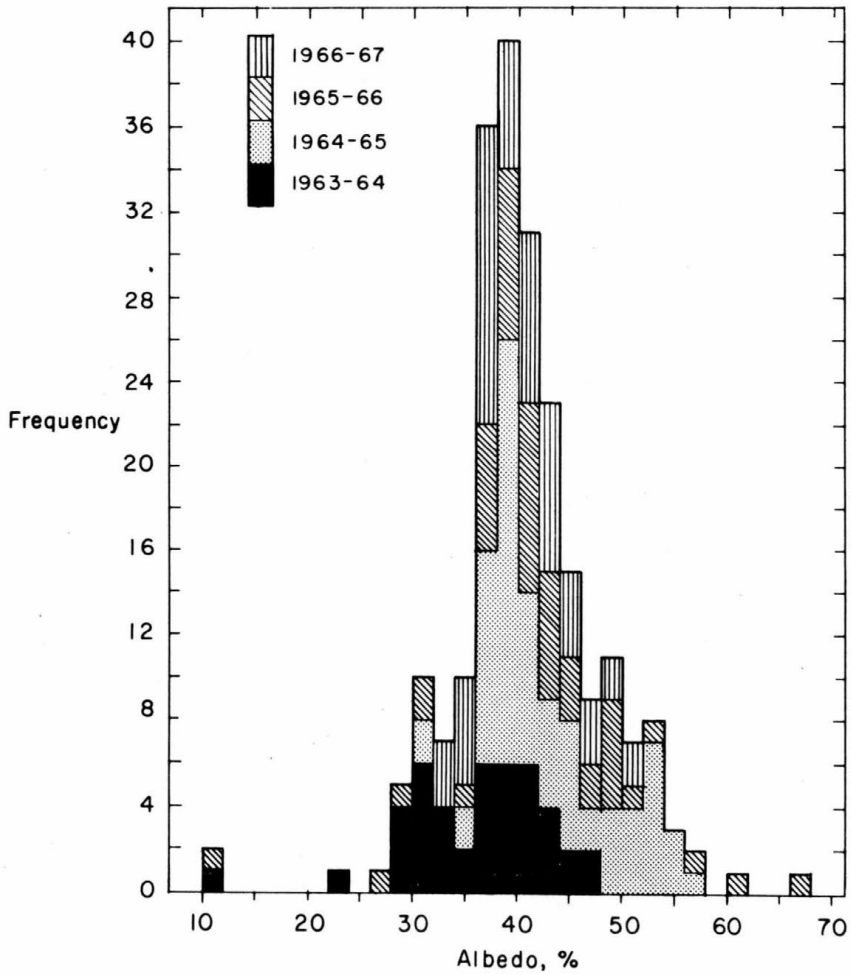

Figure 8. Albedo of slabs vs frequency.

Table V. Typical surface albedoes.

Surface type	*Albedo*
Fresh snow	0.75-0.95
Snow and ice surface	.55- .70
White brick, white paint, whitewash	.50- .70
Clouds	.40- .80
Old snow, melting ice	.40- .70
Yellow and buff brick or stone	.30- .50
Clean glacier ice	.30- .46
Sea ice	.30- .40
Entire earth	.36
Portland cement concrete, red brick, red tile, dark (red, brown, green, etc.) paints	.20- .35
Dirty glacier ice	.20- .30
Sandy soil	.15- .40
Meadows and fields	.12- .30
Tundra	.18
Forest	.05- .20
Asphalt, slate, black paint	.02- .15
Dark, cultivated soil	.07- .10
Sea water surfaces	.03- .10
Bog, muskeg	.02- .10

Since one objective of this study was to simplify computations as much as possible, daily totals were obtained from eq 10a using two techniques of accounting for albedo changes. With the first, albedoes were changed from 0.4 on days when rain or snow fell, and with the second the albedo was assumed to be 0.4 on all days. If small differences between the two techniques were apparent, the simpler method of computing quantities of absorbed shortwave radiation would obviously be to assume a constant albedo. However, cumulative totals, plotted on Figures 9-11, and differences between monthly quantities (Table VI) indicate that a significant difference exists between the two methods. Changing albedoes on days when rain or snow fell provided most accurate results. A summary of results from Table VI is:

	Monthly difference (%)			*Seasonal differences (%)*		
	Largest	*Smallest*	*Average*	*Largest*	*Smallest*	*Average*
Variable albedo	–51	–1	13	– 8	– 3	5
Constant albedo	–75	–3	23	–16	–10	14

Figures 9-11 also indicate much closer agreement with measured data when a variable surface albedo was used.

Longwave radiation

Radiation having wavelengths between 3.5 μ and 120 μ is termed longwave radiation; it includes terrestrial and atmospheric components. The radiation emitted by the earth and atmosphere has longer wavelengths than radiation emitted by the sun because the earth and atmosphere are much cooler.

Angstrom and Brunt developed equations for computing quantities of longwave radiation emitted by the atmosphere on cloudless days. Their equations are:

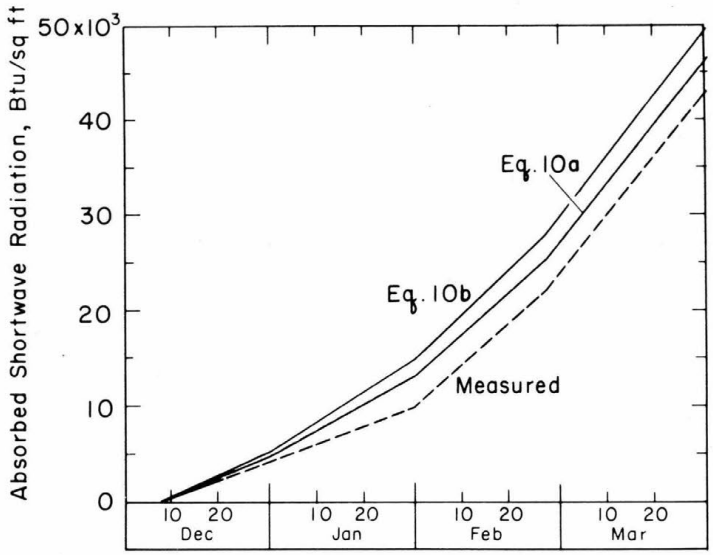

Figure 9. Absorbed shortwave radiation, 1964-1965.

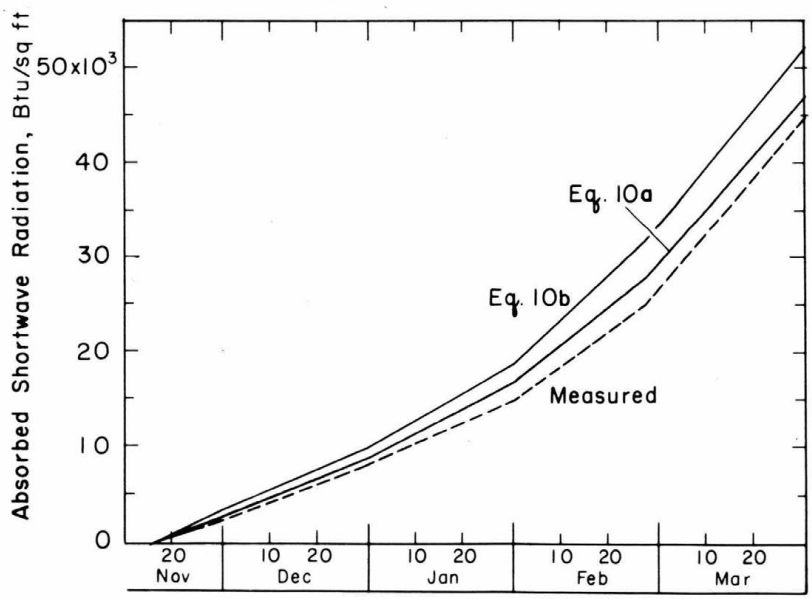

Figure 10. Absorbed shortwave radiation, 1965-1966.

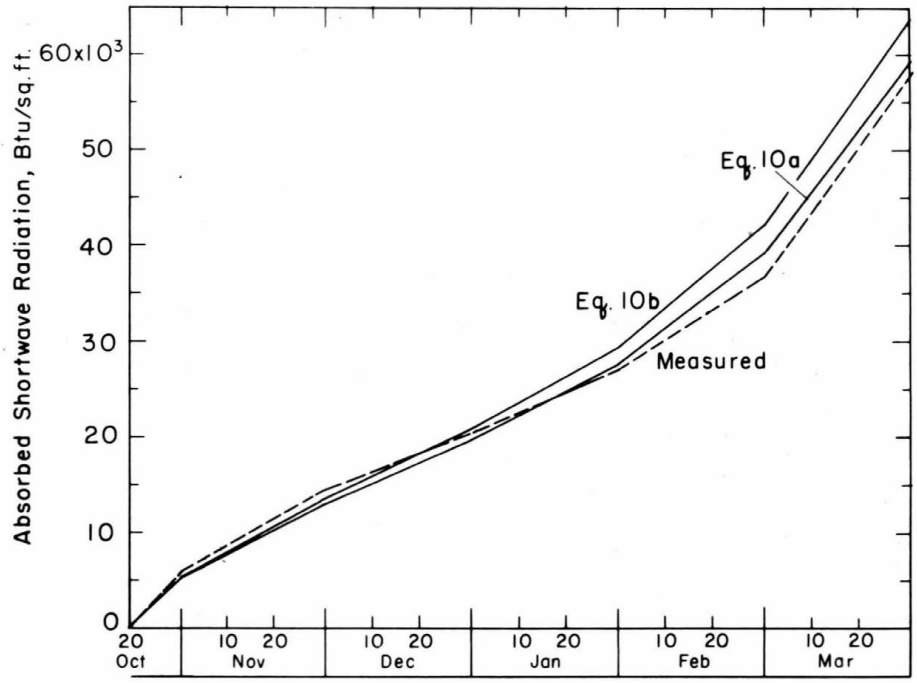

Figure 11. Absorbed shortwave radiation, 1966-1967.

$$Q_w = \sigma \epsilon_a T_a^4 \, [a - b(10^{cv})] \quad \text{(Angstrom)} \tag{11}$$

$$Q_w = \sigma \epsilon_a T_a^4 \, (d + f\sqrt{v}) \quad \text{(Brunt)} \tag{12a}$$

where

σ = Stefan-Boltzmann constant, 4.109×10^{-8} Btu/sq ft day °Rankine^4

ϵ_a = emissivity of atmosphere, dimensionless

T_a = temperature of atmosphere, °R

v = vapor pressure of atmosphere, mm of Hg

a, b, c, d and f = empirical constants.

Values for the empirical constants obtained by several investigators for different sites were shown by the Department of the Interior (1952) and extreme values for each constant from Scott (ACFEL, 1961) are given in Table VII. Quantities of longwave radiation computed from eq 11 and 12a vary considerably depending upon which constants are used. Angstrom and Brunt both assumed $\epsilon_a = 1$.

Equation 12a and constants obtained at Lake Hefner (Department of the Interior, 1952) most adequately described measured quantities of longwave radiation received at the ground surface on clear days in Lebanon. Values for d and f obtained at Lake Hefner and used at Lebanon were:

$d = 0.68$

$f = 0.036$.

Table VI. Differences between monthly totals of measured and calculated absorbed shortwave radiation (%).*

Month/method	*Variable albedo*	*Constant albedo*
	1964-1965 winter	
Dec	− 9	−21
Jan	−51	−75
Feb	+ 1	− 7
Mar	− 1	− 5
Season	− 8	−16
	1965-1966 winter	
Nov	−13	−41
Dec	− 5	−16
Jan	−23	−32
Feb	− 8	−29
Mar	+ 5	−12
Season	− 4	−16
	1966-1967 winter	
Oct	+11	+11
Nov	+ 8	+ 4
Dec	−12	−22
Jan	−19	−30
Feb	−19	−30
Mar	+ 5	− 3
Season	− 3	−10

*Difference = (measured − calculated) × (100/measured).

Table VII. Constants for Angstrom and Brunt equations (from Scott, 1969).

$$\text{Angstrom: } \frac{Q_w}{\sigma T_a^4} = a - b\,(10^{cv})$$

$$\text{Brunt: } \frac{Q_w}{\sigma T_a^4} = d + f\sqrt{v}$$

Constant	*Range*
a	0.80 -1.11
b	0.24 -0.41
c	0.022-0.163
d	0.43 -0.68
f	0.029-0.082

Examination of dry bulb and wet bulb temperature data from the Lebanon Airport Federal Aviation Administration station indicated that on most days during winter months the vapor pressure ranges between 0.0275 in. Hg and 0.138 in. Hg. Using this range of vapor pressure and values for d and f listed above, the portion of eq 12a in parentheses varies from 0.71 to 0.75 and since this variation is small a constant of 0.73 is assumed.

Using Budyko's (1958) recommended emissivity of 0.95 for the atmosphere, and the constant (0.73) obtained above from vapor pressure data, eq 12a reduces to:

$$Q_w = 2.85 \times 10^{-8} T_a^4. \tag{12b}$$

Average daily air temperatures obtained from a thermograph placed in an instrument shelter 5.2 ft above the ground surface were used as atmospheric temperatures T_a.

Table VIII contains calculated and measured (differences between measured quantities of total hemispherical and incident shortwave radiation) atmospheric radiational quantities. The range of air temperatures covered by data in Table VIII spans all but a very few air temperatures measured during the three periods of interest in this study. Calculated quantities are generally greater than measured ones, but the average of the absolute values of differences was only about 12%.

Quantities of longwave radiation emitted by the surface of the slabs were determined from the Stefan-Boltzmann law for black-body radiation:

$$Q_e = \sigma \epsilon_s T_s^4 \tag{13a}$$

where

σ = Stefan-Boltzmann constant, Btu/sq ft day $^\circ R^4$

ϵ_s = emissivity of surface, dimensionless

T_s = surface temperature, $^\circ R$.

Budyko (1958) recommends using an emissivity of 0.95 for concrete surfaces, and the value for the Stefan-Boltzmann constant is presented above. When these values are used in eq 13a, it reduces to:

$$Q_e = 3.90 \times 10^{-8} T_s^4. \tag{13b}$$

Differences between longwave radiation emitted by the slabs (outgoing) and that emitted by the atmosphere (incoming) are longwave contributions to the surface energy balance and are determined from:

$$Q_n = Q_w - Q_e \tag{14}$$

= net longwave radiation, Btu/sq ft day.

By combining eq 12b, 13b and 14, quantities of net longwave radiation on cloudless days were computed from:

$$Q_n = 2.85 \times 10^{-8} (T_a^4 - 1.37 T_s^4). \tag{15}$$

Quantities from eq 15 are compared with measured quantities obtained from:

Table VIII. Atmospheric radiation on cloudless days, winters of 1965-1966 and 1966-1967.

Date	Avg daily air temp (°F)	Calculated* (Btu/sq ft day)	Measured (Btu/sq ft day)	Difference† (%)
20 Dec 65	7.5	1359	1056	−29
4 Jan 66	21.5	1528	1376	−11
12 Jan 66	0.5	1278	1072	−19
7 Feb 66	4.2	1320	1128	−17
8 Feb 66	8.8	1373	1258	− 9
16 Mar 66	21.5	1528	1558	+ 2
21 Oct 66	43.9	1833	2012	+ 9
20 Nov 66	26.9	1598	1517	− 5
21 Nov 66	26.5	1592	1480	− 8
22 Nov 66	28.1	1614	1492	− 8
4 Dec 66	13.5	1428	1310	− 9
11 Dec 66	44.4	1840	2072	+11
6 Jan 67	9.9	1385	1332	− 4
12 Feb 67	0.1	1274	890	−43
25 Mar 67	32.8	1677	1742	+ 4
			Avg**	12

*Determined from $Q_w = 2.85 \times 10^{-8} T_a^4$

†(Measured − calculated) × (100/measured)

**Average of the absolute value of individual differences.

$$Q_a = Q_s - Q_r + Q_w - Q_e \tag{16a}$$

= net all-wave radiation, Btu/sq ft day.

Using eq 14:

$$Q_a = Q_s - Q_r - Q_n. \tag{16b}$$

Solving eq 16b for Q_n:

$$Q_n = Q_s - Q_r - Q_a. \tag{16c}$$

Measured quantities of net longwave radiation are determined from eq 16c using measured amounts of incident solar radiation, reflected solar radiation and net all-wave radiation. Calculated and measured totals of net longwave radiation on clear days are given in Table IX. No data are shown for the 1963-1964 winter because an insufficient number of temperature sensors were operating. The average of the absolute values of individual differences was 11%; but the difference between the average calculated value, −645 Btu/sq ft day, and the average measured value, −627 Btu/sq ft day, was slightly less than 3%.

Table IX. Net longwave radiation on cloudless days.

Date	Surface temp (°F)	Air temp (°F)	Calculated (Btu/sq ft day)	Measured (Btu/sq ft day)	Difference (%)
1 Jan 65	17.4	10.8	–628	–601	– 4
30 Jan 65	5.7	5.2	–491	–557	+12
20 Feb 65	13.5	6.5	–607	–541	–12
2 Mar 65	33.0	29.8	–660	–527	–25
20 Dec 65	13.4	7.5	–596	–644	+ 7
12 Jan 66	6.8	0.5	–564	–684	+18
8 Feb 66	12.2	8.8	–569	–519	–10
16 Mar 66	31.4	21.5	–741	–796	+ 7
21 Oct 66	44.5	43.9	–677	–632	– 7
13 Nov 66	38.1	30.0	–755	–685	–10
12 Dec 66	30.6	24.6	–683	–629	– 9
6 Jan 67	18.5	9.9	–645	–513	–26
25 Mar 67	40.0	32.8	–768	–742	– 4
			Avg –645	–627	11*

*Average of the absolute value of individual differences.

Net longwave radiation on cloudless days at the Lebanon Regional Airport varied from a maximum of –796 Btu/sq ft day to a minimum of –513 Btu/sq ft day, but it is not possible to establish a periodic relationship between net longwave radiation on clear days and time of year. Kondrat'yev (1965) stated that net longwave radiation varies from month to month and place to place, some locations have a maximum and a minimum, and others have several peaks. His data from four Russian sites indicated that average totals of net longwave radiation on cloudless days vary from –472 Btu/sq ft day to –937 Btu/sq ft day. Scott (1959) illustrated daily variations in net longwave radiation on clear days at Tuto, Greenland, but he recommended using a constant value of –850 Btu/sq ft day. Scott (1969) applied a constant –850 Btu/sq ft day in cumulative heat flow calculations at Thule, Greenland; Fairbanks and Kotzebue, Alaska; and Dow Air Force Base, Maine. It was therefore decided to use a constant value of –650 Btu/sq ft day for these calculations. This value is slightly greater than the average measured value, –627 Btu/sq ft day, shown in Table IX.

Net longwave radiation on cloudy days is determined from empirical equations relating it to net longwave radiation on cloudless days and average daily cloud cover (Scott, 1959; Kondrat'yev, 1965; Budyko, 1958; Sellers, 1965; Sutton, 1953). The relationships are generally quite involved and may be polynomials or may contain square root or logarithmic terms.

A polynomial regression using fifth-order to linear polynomial equations was performed on three data samples from Lebanon. In the first sample, containing slightly more than 160 pairs of data, clear day net longwave radiation was assumed a constant –650 Btu/sq ft day. In the second sample, 52 pairs of data were used and clear day net longwave radiation was determined from eq 15. In the third sample, using nearly 190 pairs of data, only longwave radiation emitted by the atmosphere was assumed to be affected by clouds; i.e., it was assumed that quantities of longwave radiation emitted by the concrete slabs were unaffected by clouds. Longwave radiation emitted by the atmosphere on clear days was determined from eq 12b and that emitted by the concrete slabs was determined from eq 13b.

In all three samples, a linear cloud-cover correction represented measured data nearly as well as more complex cloud cover correction functions. A summary of regression information is presented below (equations used to determine the correlation coefficient and standard error are in Appendix A):

Sample	Function	Correlation coefficient	Standard error
1	5th order	0.809	17.6
1	linear	.801	17.7
2	5th order	.838	16.6
2	linear	.832	16.2
3	5th order	.813	8.8
3	linear	.810	8.8

Linear equations for each sample are:

Sample 1 $$P_L = 99.5 - 7.81\, C_a \quad (17)$$

Sample 2 $$P_L = 99.2 - 7.85\, C_a \quad (18)$$

Sample 3 $$P_L = 92.4 + 3.95\, C_a \quad (19)$$

where

P_L = clear-day longwave radiation, %

C_a = average cloud cover for 24 hours, 10ths.

Daily totals of net longwave radiation were obtained from three equations:

$$Q_n = -650\,(0.995 - 0.0781\, C_a) \quad (20)$$

$$Q_n = (2.85 \times 10^{-8})\,(T_a^4 - 1.37\, T_s^4)\,(0.992 - 0.0785\, C_a) \quad (21)$$

$$Q_n = 2.85 \times 10^{-8}\, T_a^4\,(0.924 + 0.0395\, C_a) - 3.90 \times 10^{-8}\, T_s^4. \quad (22)$$

Equation 20 is the average net longwave radiation on cloudless days, –650 Btu/sq ft, multiplied by eq 17. Equation 21 is a combination of eq 15 and 18, and eq 22 combines eq 12b, 13b and 19.

Figures 12-14 show cumulative totals of net longwave radiation at the end of each month for the 1964-1965, 1965-1966 and 1966-1967 winters, respectively. Examination of the curves shows that eq 20 and 21 approximate measured totals much more closely than eq 22. Equation 21 also appears to be slightly more representative of measured data than eq 20. Table X contains differences between measured and calculated monthly totals of net longwave radiation. Differences, based on absolute values from Table X, are:

Equation	Maximum difference (%)	Minimum difference (%)	Average difference (%)
20	–43	+3	–16
21	–26	–1	–12
22	–57	+1	–23

These data and those from Figures 12-14 indicate that eq 21 most accurately predicts measured values of net longwave radiation. They also illustrate that average differences between measured and calculated net longwave radiation are nearly equal to differences in absorbed shortwave quantities (Table VI).

Table X. Differences between monthly totals of measured and calculated net longwave radiation (%).*

Month	Equations 20	21	22
1964-1965 winter			
Dec	+10	+18	+16
Jan	–43	–24	–40
Feb	+11	– 7	–23
Mar	+ 5	–11	–34
Season	– 8	– 7	–23
1965-1966 winter			
Nov	–15	–26	–57
Dec	– 5	– 1	–14
Jan	–14	–10	–30
Feb	–10	–14	–39
Mar	+27	+18	+ 1
Season	+ 2	– 1	–20
1966-1967 winter			
Oct	+14	+ 7	– 9
Nov	+16	+15	+12
Dec	–10	– 1	–10
Jan	–34	–24	–34
Feb	+ 3	+ 2	–16
Mar	+17	+ 5	–15
Season	+ 3	+ 2	–11

*Difference = (Measured – computed) × (100/measured).

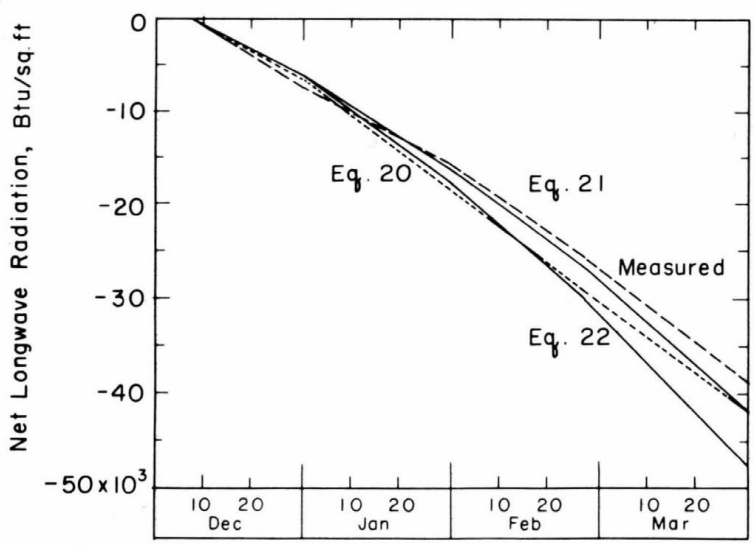

Figure 12. Net longwave radiation, 1964-1965.

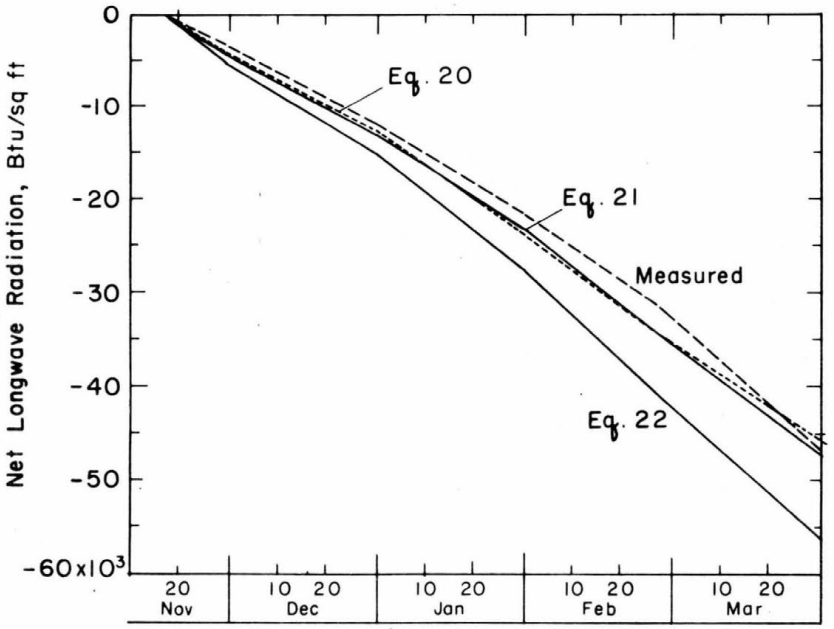

Figure 13. Net longwave radiation, 1965-1966.

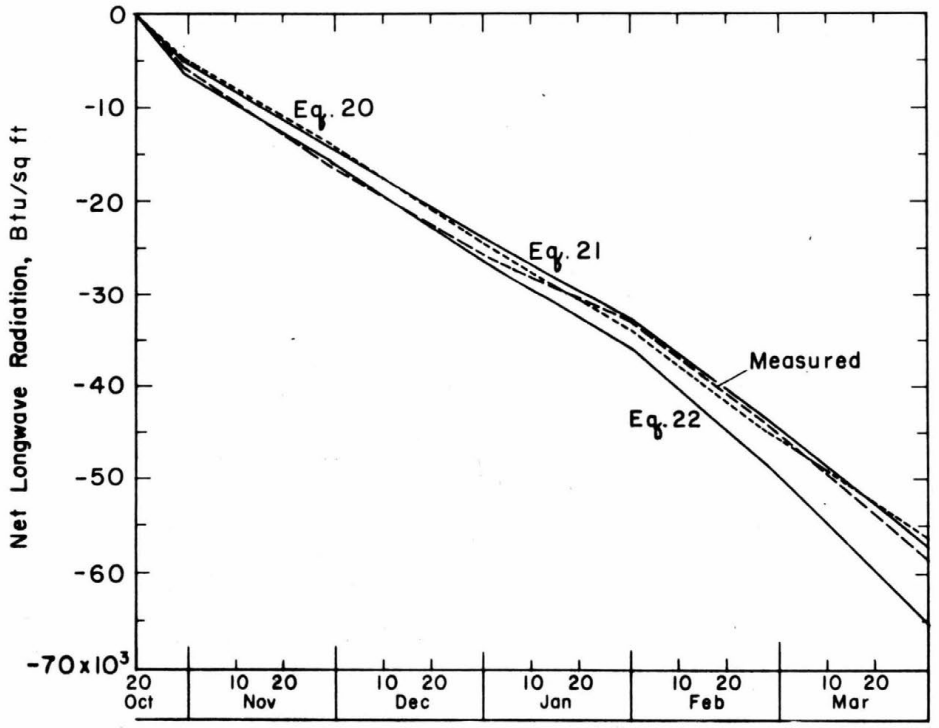

Figure 14. Net longwave radiation, 1966-1967.

Radiation balance

Equation 16a is the radiation balance equation:

$$Q_a = Q_s - Q_r + Q_w - Q_e. \tag{16a}$$

By using relationships for absorbed shortwave radiation, eq 9a, and net longwave radiation, eq 14, it reduces to:

$$Q_a = Q_{abs} - Q_n. \tag{16d}$$

From Figures 9-11 and Table VI, eq 10a:

$$Q_{abs} = (1780 + 1120 \sin \theta)(1 - A)(0.96 - 0.0071 C_d^2) \tag{10a}$$

was shown to correlate with measured quantities of absorbed shortwave radiation most closely, and Figures 12-14 and Table X indicate that eq 21:

$$Q_n = (2.85 \times 10^{-8})(T_a^4 - 1.37 T_s^4)(0.992 - 0.0785 C_a) \tag{21}$$

most closely represented measured totals of net longwave radiation. In Table XI, the radiation balance, determined by combining data from Figures 9-14, is tabulated for each month during the three winters. Measured monthly values of the radiation balance and differences between measured and calculated quantities are also shown in Table XI.

Differences between measured and calculated quantities of the monthly radiation balance are much greater than differences obtained when absorbed shortwave and net longwave radiation quantities are computed individually (Tables VI and X). Large differences exist because the quantities of absorbed shortwave radiation and net longwave radiation are approximately of the same magnitude but of opposite sign. Therefore, relatively small errors in computing either or both of these quantities are magnified and much larger errors result when the radiation balance is determined.

Table XI. Radiation balance – monthly totals.

	1964-1965			*1965-1966*			*1966-1967*		
Month	*Calculated** *(Btu/sq ft)*	*Measured (Btu/sq ft)*	*Difference†* *(%)*	*Calculated** *(Btu/sq ft)*	*Measured (Btu/sq ft)*	*Difference†* *(%)*	*Calculated** *(Btu/sq ft)*	*Measured (Btu/sq ft)*	*Difference* *(%)*
Oct							+ 91	+ 331	+ 72
Nov				−1806	−1223	−48	−1483	−2426	+ 39
Dec	−1532	−3232	+53	−2589	−2804	+ 8	−2682	−3301	+ 19
Jan	−1899	−2749	+31	−2253	−2860	+21	−1064	− 610	− 74
Feb	+1550	+2346	+34	+ 339	+ 587	+93	+1011	−1066	+195
Mar	+6420	+7503	+14	+6268	+4613	+36	+6071	+6269	+ 3
Total	+4539	+3868	−15	− 341	−1687	+80	+1944	− 803	+348

*Calculated from data in Figures 9-14.

†(Measured − calculated) × (100/measured). Average monthly difference = 49%.

An example of relatively small differences between measured and calculated quantities of net longwave and absorbed shortwave radiation becoming large when the two components are combined is the quantity for February 1967. The calculated absorbed shortwave total from Table VI was 19% greater than the measured total and the calculated net longwave total from Table X was 2% less than the measured total. However, the measured radiation balance from Table XI was 195% less than the calculated total.

In the ensuing calculations and discussions, calculated data in Table XI were used as the radiation balance.

Convection

Energy balance components due to convection and conduction into the air are extremely difficult to measure accurately in field studies (Sellers, 1965a) and are nearly impossible to measure individually. Analytical techniques for approximating the parameters are available (Bird *et al.*, 1960; ASHRAE, 1961; Budyko, 1958; Department of the Interior, 1952; Department of the Navy, 1955; Dingman *et al.*, 1968; Geiger, 1965; Sutton, 1953; Deacon, 1949; Sellers, 1965; Scott, 1969, 1970a, b). Since few correlations between analytical and experimental data were available, choosing the most acceptable analytical method was difficult.

As stated in the section *General equation*, the thermal conductivity of air is very small, so heat transfer by conduction into the air was neglected.

Heat flux by convection is calculated from:

$$Q_c = h(T_a - T_s) \tag{23}$$

where

h = heat transfer coefficient, Btu/sq ft day °F.

The heat transfer coefficient is the most difficult quantity to define in eq 23, and Bird *et al.* (1960) indicate that for gases it is generally between 24 Btu/sq ft day °F and 480 Btu/sq ft day °F. They state, "The heat-transfer coefficient depends in a complicated way on many variables, including the fluid properties ..., the system geometry, the flow velocity, the value of the characteristic temperature difference, and the surface temperature distribution."

Scott (1970a) simplifies an equation proposed by Deacon (1949) and determines heat transfer coefficients as a function of wind speed about 5 ft above the ground surface from:

$$h = 5.5u \tag{24}$$

where

u = wind speed, mph.

Empirical equations obtained from the literature are:

$$h = 16 + 7.7u \text{ (ASHRAE, 1961)} \tag{25}$$

$$h = (9.1 + 2.3u)(T_a - T_s)^{0.25} \text{ (Department of the Navy, 1955).} \tag{26}$$

Sellers (1965) presented an aerodynamic equation for vertical heat flux by convection when wind velocity increases logarithmically with height:

$$Q_c = \rho c_p k^2 \left[\frac{\Delta u \Delta T}{\ln (Z_2/Z_1)^2}\right] \tag{27}$$

where

ρ = density of air, lb/cu ft

c_p = specific heat at constant pressure, Btu/lb °F

k = von Karman's constant, dimensionless

Δu = difference in wind speed between heights Z_1 and Z_2 above surface, ft/day

ΔT = temperature difference between heights Z_1 and Z_2 above surface, °F.

Although the wind velocity often does not vary logarithmically with height, eq 27 was investigated and compared with eq 24-26.

Rearranging terms in eq 27 indicates the heat transfer coefficient is:

$$h = \rho c_p k^2 \left[\frac{\Delta u}{\ln (Z_2/Z_1)^2}\right]. \tag{28}$$

The roughness height indicates irregularities in the surface and wind velocities are assumed equal to zero at this level (Sellers, 1965). Assuming Z_1 is equal to the roughness height of 0.0003 ft (0.01 cm) used by Scott (1969, 1970a, b), Z_2 is 5.25 ft (160 cm) above the ground, the density of air is 0.08 lb/cu ft (Lange, 1961), the specific heat of air is 0.24 Btu/lb °F (Lange, 1961), and von Karman's constant is 0.4, the heat transfer coefficient from eq 28 is:

$$h = 4.1u \tag{29}$$

where u is the wind velocity at about 5.25 ft above the surface in miles per hour. The density and specific heat of air change slightly with temperature; values given above are for air at 32°F but differences of ±20°F produce changes of less than 10% in eq 29.

A comparison of measured surface and air temperatures for these three winters indicated that the surface averaged approximately 3°F warmer than the air temperature. If this difference is used in eq 26, it reduces to:

$$h = 12 + 3.0u. \tag{30}$$

Heat transfer coefficients determined from eq 24, 25, 29 and 30 vary over such a wide range, under similar conditions, that heat flux was calculated from two equations. It is obvious that eq 29 provides the lowest heat transfer coefficients and eq 25 provides the highest. Therefore, eq 29 and 25, respectively, were combined with eq 23 and two expressions for heat flux by convection were provided:

$$Q_c = 4.1u\,(T_a - T_s) \tag{31}$$

$$Q_c = (16 + 7.7u)\,(T_a - T_s). \tag{32}$$

Heat flux by convection was not measured independently in this study; instead, heat fluxes by mechanisms other than radiation and conduction into the ground were combined and determined as a residual from the energy balance equation (eq. 2). These residuals are discussed in the next section.

Condensation, evaporation, evapotranspiration and sublimation

These parameters are difficult to measure accurately and are often neglected when energy balances over paved surfaces are computed (Scott, 1969, 1970a). Evapotranspiration was not considered because no vegetation grew on the slabs and condensation was eliminated by assuming that energy added by condensation was lost when the condensate evaporated.

Sublimation of snow remaining after snow removal may affect the surface energy balance; however, probably only a very thin layer remained because the slabs were shoveled and swept after each storm. A layer of snow equal to the roughness of the slabs, 10^{-2} ft to 10^{-3} ft (Rouse, 1946) was assumed to remain and the quantity of heat required for sublimation of this layer was:

$$Q_l = \Delta s \rho_s \frac{H_s}{t} \tag{33}$$

where

Δs = thickness of snow layer, ft

ρ_s = density of snow, lb/cu ft

H_s = heat of sublimation at 32°F, Btu/lb

t = time, day.

Using a layer thickness of 0.005 ft, a density of 18 lb/cu ft (Mellor, 1964), and heat of sublimation of 1220 Btu/lb (Mellor, 1964), and assuming all the snow sublimes the day it falls, heat flux by sublimation was –110 Btu/sq ft after each snow storm. An equal quantity of heat was assumed to be transferred by evaporation after a rain storm.

Since evaporation and sublimation on paved surfaces are sometimes neglected, heat fluxes by these mechanisms are computed in two different ways. In the first, a heat flux of –110 Btu/sq ft is assumed on days of rainfall or snowfall; and in the second, heat fluxes by evaporation and sublimation are neglected throughout the periods studied.

As indicated in the previous section, heat fluxes by convection, sublimation and evaporation are not measured individually but are determined as the residual in the energy balance equation (eq 2) or:

$$Q_c + Q_l = Q_s - Q_r + Q_w - Q_e - Q_g. \tag{2a}$$

Using eq 16a:

$$Q_c + Q_l = Q_a - Q_g. \tag{34}$$

Heat flux by convection, evaporation and sublimation was calculated in three ways using these equations:

$$Q_c + Q_l = (16 + 7.7u)(T_a - T_s) \tag{32}$$

$$Q_c + Q_l = (16 + 7.7u)(T_a - T_s) - 110 \tag{35}$$

$$Q_c + Q_l = 4.1u(T_a - T_s). \tag{31}$$

The three techniques used to compute heat flux by these parameters are: 1) eq 32 used on all days; 2) eq 35 used on days of rainfall or snowfall and eq 32 used on other days; and 3) eq 31 used on all days. Cumulative totals of measured quantities, obtained from eq 34, and calculated data are shown in Figures 15-17. Monthly differences are shown in Table XII. Differences are summarized below:

Equation	*Maximum difference (%)*	*Minimum difference (%)*	*Average difference (%)*
32	–2458	+45	–572
32&35	–2802	+45	–725
31	– 821	+ 5	–192

All of the monthly differences between measured and calculated data are extremely large. It is evident that heat transfer by convection, evaporation and sublimation is not calculated accurately using these equations. More complex equations are necessary to reflect the complicated physical processes involved in these energy balance components.

Table XII. Differences between monthly totals of measured and calculated convection, evaporation and sublimation (%).*

	Equations		
Month	*32*	*32&35*	*31*
	1964-1965 winter		
Dec	+ 176	+ 229	+130
Jan	– 64	– 138	+ 41
Feb	– 197	– 255	– 8
Mar	– 148	– 161	+ 5
Season	– 236	– 296	– 27
	1965-1966 winter		
Nov	– 231	– 304	– 17
Dec	+1321	+1620	+536
Jan	–1832	–2322	–597
Feb	–2458	–2802	–821
Mar	– 238	– 281	– 31
Season	– 647	– 765	–174
	1966-1967 winter		
Oct	+ 45	+ 45	+ 82
Nov	+ 710	+1185	+335
Dec	– 75	– 156	+ 49
Jan	– 153	– 287	+ 30
Feb	– 773	– 907	–173
Mar	– 163	– 185	+ 15
Season	– 218	– 284	– 1

*Differences = (Measured – calculated) × (100/measured).

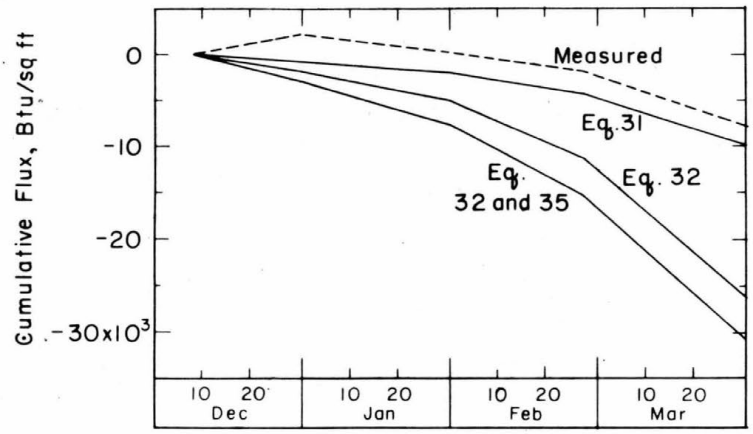

Figure 15. Convection, evaporation and sublimation, 1964-1965.

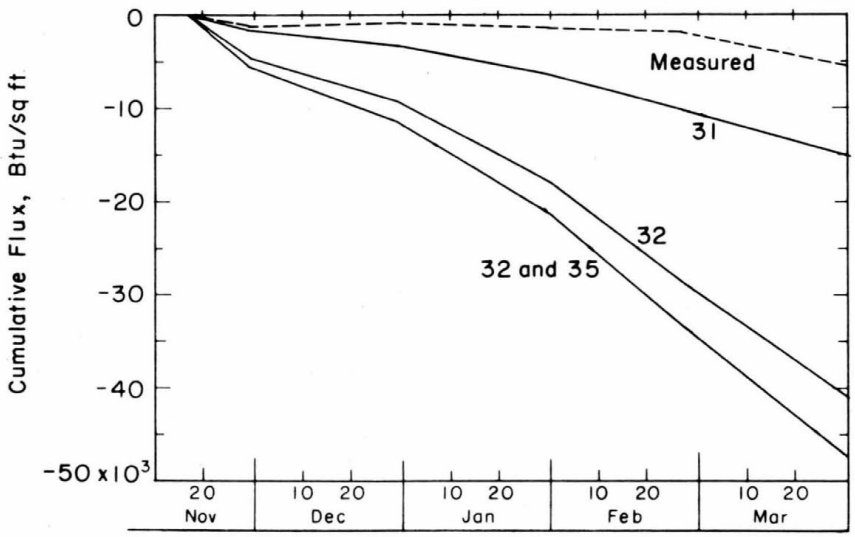

Figure 16. Convection, evaporation and sublimation, 1965-1966.

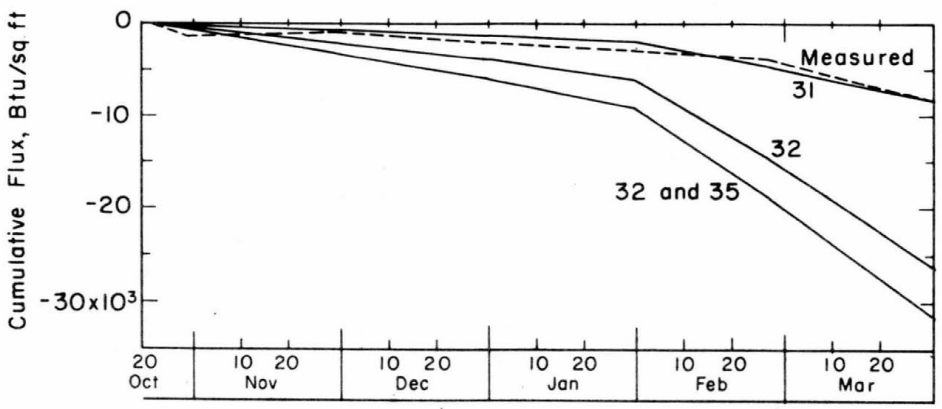

Figure 17. Convection, evaporation and sublimation, 1966-1967.

Conduction into the ground

Measured quantities of heat flux into the ground by conduction were not obtained directly but were computed from measured subsurface temperatures as explained in Appendix C. Calculated quantities were obtained from the most accurate technique used to compute each surface energy balance component and these techniques were then combined in eq 2:

$$Q_g = Q_s - Q_r + Q_w - Q_e \pm Q_c \pm Q_l \tag{2}$$

to determine heat flux into the ground.

As discussed in the preceding sections, the most accurate mathematical techniques were:

$$Q_s - Q_r = Q_{abs} = (1780 + 1120 \sin \theta)(1 - A)(0.96 - 0.0071\, C_d^2) \tag{10}$$

$$Q_w - Q_e = Q_n = (2.85 \times 10^{-8})(T_a^4 - 1.37\, T_s^4)(0.992 - 0.0785\, C_a) \tag{21}$$

$$Q_c = 4.1u\,(T_a - T_s) \tag{32}$$

$$Q_l = 0. \tag{36}$$

A computer program was written to compute cumulative daily sums of Q_g from eq 2 using eq 10, 21, 32 and 36. The program listing and data obtained from the computer are in Appendix D.

Comparisons of measured and calculated quantities of heat flux into the ground are shown in Figures 18-20, and Table XIII contains differences between measured and calculated monthly quantities. It should be noted that the figures depict cumulative monthly totals, whereas data in the table are based on monthly totals. Data in Table XIII indicate that the maximum monthly difference is 2320%, the minimum monthly difference is 7%, and the average monthly difference is 223%. Monthly differences are somewhat compensating; thus seasonal differences are smaller than monthly differences. Seasonal differences between measured and calculated quantities were –36% for 1964-1965, 30% for 1966-1967, but –114% for the 1965-1966 winter. The reason for the large difference in 1965-1966 was numerically large quantities in December and January as indicated in Figure 19.

All of the differences are much greater than acceptable levels; this is discussed in the next section.

Table XIII. Differences between monthly totals of measured and calculated conduction into the ground (%).*

Month	*1964-1965*	*1965-1966*	*1966-1967*
Oct			+86
Nov		– 32	+ 8
Dec	–134	– 78	+26
Jan	+ 35	– 62	– 7
Feb	+403	+2320	+18
Mar	+ 54	– 54	–25
Season	– 36	– 114	+30

Average monthly difference = –223%

*Difference = (Measured – calculated) × (100/measured).

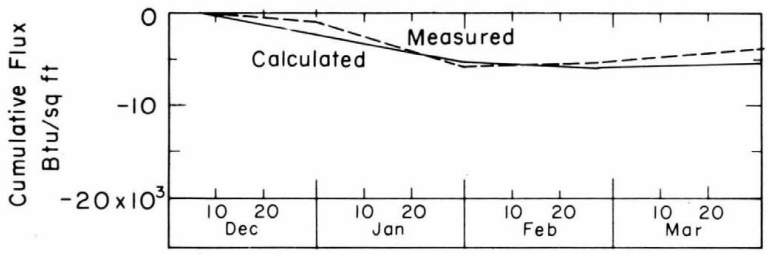

Figure 18. Conduction into the ground, 1964-1965.

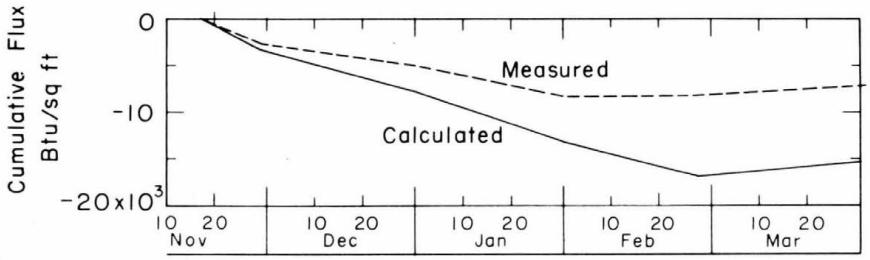

Figure 19. Conduction into the ground, 1965-1966.

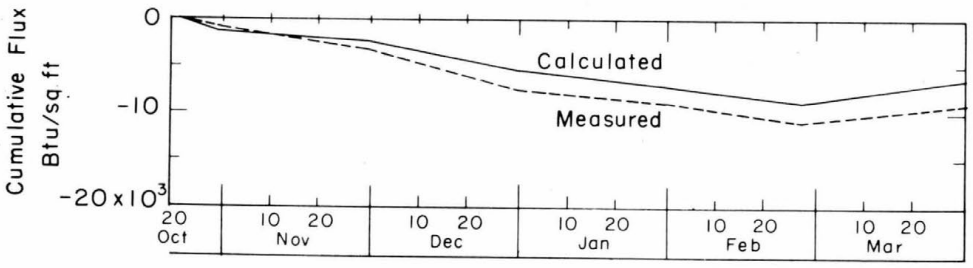

Figure 20. Conduction into the ground, 1966-1967.

DISCUSSION

Three techniques for computing frost or thaw penetration depths were discussed in the section *Frost and thaw depths* (p. 6); all three require that an upper (surface) boundary condition be defined. The most simple method of defining the surface condition is to assume that the air and surface temperatures are equal. However, previous experience, especially with asphaltic concrete and portland cement concrete pavements, indicated that the relationship was not so simple. By using measured air and surface indexes, empirical *n*-factors relating them have been obtained. Those currently used for design purposes were published by the Departments of the Army and the Air Force (1966a).

The necessity for improving methods of estimating surface temperatures has been recognized for some time. Scott (1959) was among the first to use micrometeorological data for this purpose.

In his studies, Scott (1969, 1970a, b; ACFEL, 1961) developed a cumulative heat flux technique for computing frost and thaw depths. Scott's procedures, or refinements of them, are used for computations of the surface energy balance outlined in the preceding sections of this report.

As indicated in the section, *Frost and thaw depths* (p. 6), input data currently used with the modified Berggren equation provide calculated frost or thaw depths which are generally within ±15% of measured depths. If the accuracy is not improved by using the surface energy balance with Scott's cumulative heat flow technique or another method, the existing method (the modified Berggren equation) for computing frost and thaw depths will remain most desirable since input data are easily attained and have been studied in considerable detail (Sanger, 1963).

Scott's (1969, 1970a, b) technique was used to construct a working curve (Fig. 21) relating frost penetration and cumulative heat flux into the ground to illustrate the consequence of 10% errors on computed frost depths at Lebanon Regional Airport. Using cumulative heat fluxes with Figure 21, it was evident that, at this site, 10% differences in cumulative heat flux resulted in computed frost depths that were also approximately 10% different. Some typical examples are:

Q_{g1}	Q_{g2}	Q	X_1	X_2	X
– 2,000	– 2,200	10%	1.50	1.65	10%
– 5,000	– 5,500	10%	3.45	3.80	10%
–12,000	–13,200	10%	7.75	8.45	9%

Q_{g1} = heat flux into ground, example 1, Btu/sq ft

Q_{g2} = heat flux into ground, example 2, Btu/sq ft

Q = heat flux difference, %

X_1 = frost depth, example 1, ft

X_2 = frost depth, example 2, ft

X = frost depth difference, %.

For soils with thermal properties different from those at Lebanon, 10% errors may cause slightly greater or slightly smaller errors in computed frost depths. Investigation of Scott's (1969, 1970a, b) data shows changes in computed frost and thaw depths of 2% to 25% for 10% changes in cumulative heat flux.

From the preceding discussion, it is evident that differences between measured and calculated surface energy balance totals must be less than ±15% to be acceptable.

To obtain this accuracy in radiation balance calculations, monthly differences in quantities of net longwave and/or absorbed shortwave radiation must be reduced. The average monthly errors for net longwave and absorbed shortwave radiation were 12% and 13%, respectively, and the average monthly error in radiation balance calculations was 49%. Assuming that monthly differences in the radiation balance remain three to four times greater than monthly differences of net longwave or absorbed shortwave radiation, the 12% and 13% quantities must be calculated with average differences of 5% or less. Most of the errors in computing the radiation balance can be attributed to inadequate relationships between cloud cover and radiation balance components. It appears that these relationships can be defined only with more sophisticated instrumentation than that used at the Lebanon site. In the future, satellites may provide measurements of the radiation balance at any location on the earth (Rados, 1967).

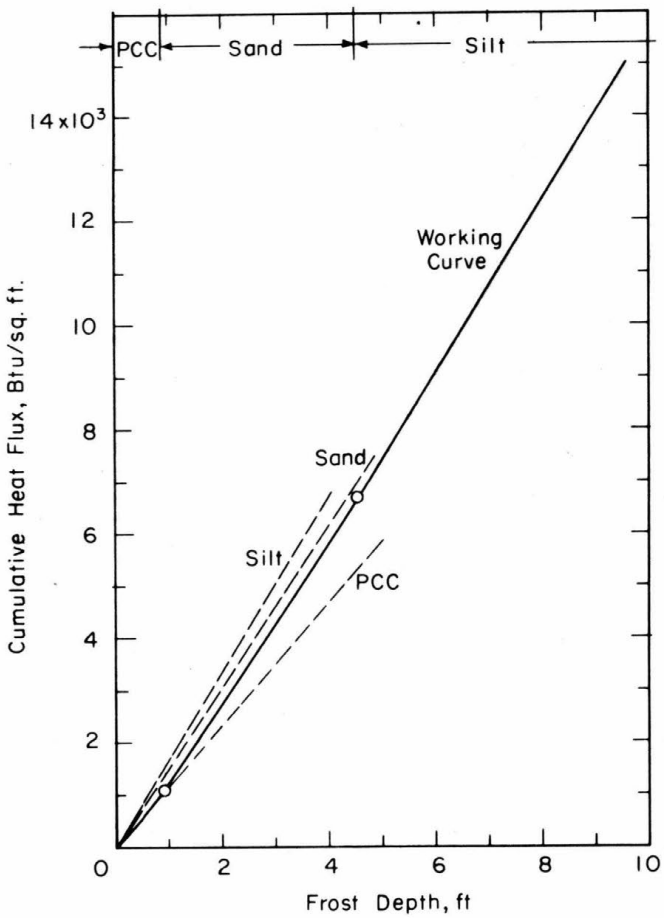

Figure 21. Cumulative heat flux vs frost depth.

Calculating heat losses by convection is a major problem. In most studies of heat losses by convection, a large, flat, bare or vegetated area free from trees and other obstacles causing disturbances in air flow was chosen (Sellers, 1965b); results from previous studies have not provided adequate computational techniques. Since roads and runways are of various widths and may be located in a cut or a fill area or may be surrounded by trees, grass or snow of various heights and depths, the possibilities of estimating their heat flux by convection appear remote if relatively simple relationships are desired.

Because surfaces considered in this study were paved, heat flows by mass movement of water through the soil and by evapotranspiration were neglected, but over unpaved surfaces these two modes of heat transfer may be very important. One technique for computing evaporative (evapotranspiration) losses from natural soil and water surfaces is the Bowen ratio, defined as:

$$B = \frac{Q_c}{Q_1}. \tag{37}$$

It relates heat lost by convection with that lost by evaporation and is often used (Department of Interior, 1952; Dingman *et al.*, 1968; Geiger, 1965; Sellers, 1965a, b; Sutton, 1953). According to Sellers' (1965a) data for land surfaces, the Bowen ratio varies from 0.56 to 2.18 with an average value of 0.96. A more complete discussion of this ratio is in the references cited above.

Other recent energy balance studies also indicate that a more thorough understanding of the processes of convective and evaporative heat losses is desirable. Dingman *et al.* (1968) conclude that a limited understanding of these phenomena reduces the accuracy of their computations. Sellers (1965b) used an equation similar to eq 34 to determine convective losses. He measured Q_g and Q_n and used these data and eq 34 to test current theories of forced and free convection at the air/ground interface. In analyzing these data, Sellers and Dryden (1967) obtain an empirical equation representative of the data; however, it is much more complex than eq 31 and 32 and they indicate that additional work is necessary to validate it.

The two primary difficulties with the surface energy balance concept used here are that several of the components were computed from empirical rather than theoretical equations and relatively simple relationships were used to minimize the number of input variables. Empirical relationships were used because they were often the only ones available. The number of variables was minimized because those requiring sophisticated instrumentation are not measured at many of the weather stations; therefore, they are difficult to estimate reliably due to insufficient data collection sources.

CONCLUSIONS

Relatively small differences between computed and measured quantities of absorbed shortwave and net longwave radiation become much larger when the components are combined into the radiation balance. Additional parameters must be considered to reduce computational errors in the radiation balance to an acceptable level.

Heat lost by the combined fluxes of convection, evaporation and sublimation is nearly 225% different from measured values and causes the greatest portion of error between calculated and measured heat fluxes out of the ground.

Relatively simple relationships were used to calculate the surface energy balance components. This approach was taken to determine the accuracy of the procedure for the design of facilities at remote locations where limited data are available. Computed values of the energy balance components were inaccurate, indicating the need for more complex relationships. The more complex relationships will probably require too many parameters to be adopted for design purposes; therefore it appears desirable to continue using *n*-factors for most design studies. The energy balance procedure may be applied at sites where sufficient information is available to allow the use of more sophisticated equations.

RECOMMENDATIONS

Since the *n*-factors currently used were determined from a limited amount of data, a study incorporating information from several more locations and for more than one year should be conducted. In such a study it would be possible to examine the effects of all or some of these factors: latitude, elevation, exposure, wind speed, incident shortwave radiation, type of surface, and average degree of cloudiness.

LITERATURE CITED

Aldrich, H.P. and Paynter, H.M. (1953) Analytical studies of freezing and thawing of soils. First Interim Report. U.S. Army Arctic Construction and Frost Effects Laboratory (USA ACFEL) Technical Report 42.

American Society of Heating, Refrigerating and Air-Conditioning Engineers, Inc. (ASHRAE) (1961) *Guide and data book, fundamentals and equipment.* New York: ASHRAE.

Berg, R.L. (1973) Thermo-insulating media within embankments on perennially frozen soil. Ph.D. thesis, University of Alaska, Fairbanks, Alaska.

Bird, R.B.; Stewart, W.E. and Lightfoot, E.N. (1960) *Transport phenomena.* New York: John Wiley and Sons, Inc.

Bolsenga, S.J. (1964) Daily sums of global radiation for cloudless skies. U.S. Army Cold Regions Research and Engineering Laboratory (USA CRREL) Research Report 160 (AD 610552).

Budyko, M.I. (1958) The heat balance of the earth's surface. Translated by N.A. Stepanova, Department of Commerce, Washington, D.C.

_____, Editor (1963) Atlas of the heat balance of the earth. Academy of Science, USSR, Moscow, Translated by I.A. Donehoo, U.S. Weather Bureau.

Byers, H.R. (1959) *General meteorology,* Third edition. New York: McGraw-Hill Book Co., Inc.

Deacon, E.L. (1949) Vertical diffusion in the lowest layers of the atmosphere. *Quarterly Journal of the Royal Meteorological Society,* vol. 75.

Department of the Army (1965) Pavement design for frost conditions. TM 5-818-2. (Department of the Air Force Manual AFM 88-6, Chapter 4.)

Department of the Army (1966a) Arctic and subarctic construction - calculation methods for determination of depths of freeze and thaw in soil. TM 5-852-6 (Department of the Air Force Manual AFM 88-19, chapter 6).

_____ (1966b) Arctic and subarctic construction - General provisions. TM 5-852-1 (Department of the Air Force Manual AFM 88-19, chapter 1).

Department of the Interior (1952) Water-loss investigations: Vol. 1 - Lake Hefner studies. Technical Report, Geological Survey Circular 229.

Department of the Navy (1955) Arctic engineering. Technical Publication NAVDOCKS TP-PW-11.

Dingman, S.L.; Weeks, W.E. and Yen, Y.C. (1968) The effects of thermal pollution on river ice conditions. *Water Resources Research,* vol. 4, no. 2, p. 349-362.

Dusinberre, G.M. (1961) *Heat transfer calculations by finite differences.* Scranton, Pa.; International Textbook Company.

Eppes, R., Jr. (1966) Solution of transient heat transfer problems for flat plates, cylinders, and spheres by finite-difference methods with application to surface recession. U.S. Army Missile Command, Redstone Arsenal Report No. RS-TR-66-4.

Fuquay, D. and Buettner, K. (1957) Laboratory investigation of some characteristics of the Eppley pyrheliometer. *Transactions of the American Geophysical Union,* vol. 38, no. 1, p. 38-43.

Geiger, R. (1965) *The climate near the ground.* Translated by Scripta Technica, Inc., Cambridge, Mass.: Harvard University Press.

Gerdel, R.W.; Diamond, M. and Walsh, K.S. (1954) Monographs for computation of radiation heat supply. U.S. Army Snow, Ice and Permafrost Research Establishment (USA SIPRE) Research Paper 8 (AD 31051).

Gier, J.T. and Dunkle, V.R. (1951) A hemispherical radiometer. *Transactions of the American Institute of Electrical Engineers,* vol. 70, Part 1.

Kersten, M.S. (1949) Laboratory research for the determination of the thermal properties of soils. USA ACFEL Technical Report 23.

LITERATURE CITED (Cont'd)

Klein, W.H. (1948) Calculation of solar radiation and the solar heat load on man. *Journal of Meteorology,* vol. 5, no. 4, p. 119-129.

Kondrat'yev, K.Y. (1965) *Radiative heat exchange in the atmosphere.* Translated by O. Tedder. New York: Pergamon Press, Inc.

Lange, N.A. (1961) *Handbook of chemistry.* 10th edition. New York: McGraw-Hill Book Co., Inc.

List, R.J. (1963) Smithsonian meteorological tables, Sixth Revised Edition. Smithsonian Institution, Washington, D.C.

Mellor, M. (1964) Properties of snow. USA CRREL, Cold Regions Science and Engineering Monograph III-A1 (AD 611023).

Rados, R.M. (1967) The evolution of the TIROS meteorological satellite operational system. In *Bulletin of the American Meteorological Society,* vol. 48, no. 5, p. 326-337.

Rouse, H. (1946) *Elementary mechanics of fluids.* New York: John Wiley and Sons, Inc.

Sanger, F.J. (1963) Degree-days and heat conduction in soils. In *Proceedings, Permafrost International Conference.* National Academy of Science - National Research Council.

Scott, R.F. (1959) Study and report of micrometeorological data obtained in 1957-1958 at Tuto, Greenland, USA ACFEL Contract Report.

_____ (1963) Factors affecting freezing or thaw depth in soils. In *Proceedings, Permafrost International Conference.* National Academy of Sciences - National Research Council.

_____ (1969) Predicted depths of freeze or thaw in soils by climatological analysis of cumulative heat flow. USA CRREL Technical Report 195 (AD 696414).

_____ (1970a) Validation of the cumulative heat flow technique. USA CRREL Technical Report 200.

_____ (1970b) Study of cumulative heat flow. USA CRREL Technical Report 201.

Sellers, W.D. (1965a) *Physical climatology.* Chicago, Illinois: The University of Chicago Press.

_____ (1965b) An investigation of heat transfer from bare soil. Final Report, Prepared under Grant No. DA-AMC-28-043-65-G-11, for Meteorology Department, U.S. Army Electronic Proving Ground, Ft. Huachuca, Arizona.

_____ and Dryden, P.S. (1967) An investigation of heat transfer from bare soil. Final Report, Prepared under Grant No. DA-AMC-28-043-66-G27, for Meteorology Department, U.S. Army Electronic Proving Ground, Ft. Huachuca, Arizona.

Sutton, O.G. (1953) *Micrometeorology.* New York: McGraw-Hill Book Co., Inc.

U.S. Army Arctic Construction and Frost Effects Laboratory (USA ACFEL) (1961) Heat transfer at the air-ground interface with special reference to airfield pavements. (Massachusetts Institute of Technology, Contract no. DA-19-016-ENG-2743) Technical Report 63.

U.S. Department of Commerce (1963-1967a) Climatological data for New England (monthly summaries). Environmental Science Services Administration, Weather Bureau.

_____ (1963-1967b) Climatological data (National summary, September 1963-April 1967). Environmental Science Services Administration, Weather Bureau.

Wilson, C. (1967) Climatology of the cold regions, Introduction: Northern Hemisphere I. USA CRREL, Cold Regions Science and Engineering Monograph I-A3a (AD 656460).

APPENDIX A. EQUATIONS FOR CORRELATION COEFFICIENT AND STANDARD ERROR

Correlation coefficient:

$$R = \frac{\Sigma xy - (\Sigma x \Sigma y/n)}{\{[\Sigma x^2 - (\Sigma x)^2/n]\,[\Sigma y^2 - (\Sigma y)^2/n]\}^{1/2}}$$

Standard error:

$$S = \frac{[\Sigma y^2 - (\Sigma y)^2/n]\,[1 - R^2]}{n - 2}$$

where

x = value of independent variable

y = value of dependent variable

n = sample size.

For the regression in this report, the cloud cover was considered the independent variable and the percentage of possible clear-day radiation was deemed the dependent variable.

APPENDIX B. MEASURED RADIATION ON CLOUDLESS DAYS

Table BI. Measured radiation on cloudless days.

Heat flux by net all-wave radiation and heat flux by net longwave radiation were not computed for all days because cloud cover for 24-hour period was not zero.

Date	Cloud cover 24 hours 10ths	Cloud cover daylight hours 10ths	Heat flux by incident shortwave radiation (Btu/sq ft day)	Heat flux by reflected shortwave radiation (Btu/sq ft day)	Heat flux by net all-wave radiation (Btu/sq ft day)	Heat flux by net longwave radiation (Btu/sq ft day)
16 Dec 63	0	0	+ 866	− 411	−396	−851
28 Dec 63	1	0	+ 858	− 452		
30 Dec 63	0	0	+ 888	− 363	−252	−777
11 Jan 64	1	0	+ 918	− 373		
15 Jan 64	0	0	+ 943	− 474	−107	−576
3 Feb 64	0	0	+1160	− 512	−174	−822
9 Feb 64	1	0	+1269	− 497		
11 Feb 64	0	0	+1320	− 510	+ 35	−775
12 Feb 64	0	0	+1322	− 506	+ 97	−719
23 Feb 64	0	0	+1575	− 616	+277	−682
29 Feb 64	1	0	+1616	− 592		
20 Mar 64	0	0	+2143	− 660	+546	−937
23 Mar 64	1	0	+2198	− 679		
1 Nov 64	1	0	+1021	− 526		
2 Nov 64	0	0	+ 979	− 520	− 12	−471
4 Nov 64	0	0	+ 989	− 529	− 14	−474
14 Nov 64	2	0	+ 884	− 480		
15 Nov 64	2	0	+ 822	− 414		
29 Dec 64	3	0	+ 706	− 419		
1 Jan 65	0	0	+ 737	− 386	−250	−601
6 Jan 65	2	0	+ 727	− 413		
21 Jan 65	2	0	+ 869	− 629		
30 Jan 65	0	0	+1003	− 729	−283	−557
17 Feb 65	1	0	+1268	− 523		
20 Feb 65	0	0	+1363	− 638	+184	−541
23 Feb 65	0	0	+1416	− 673	+181	−562
2 Mar 65	0	0	+1444	− 444	+473	−527
12 Mar 65	1	0	+1646	− 670		
24 Mar 65	1	0	+1834	− 699		
31 Mar 65	0	0	+2016	−1691	M*	M
3 Apr 65	0	0	+1992	− 768	M	M
4 Apr 65	0	0	+2017	− 788	M	M
19 Oct 65	1	0	+1070	− 397		
20 Dec 65	0	0	+ 705	− 345	−284	−644

*M = Data missing.

Table BI (Cont'd). Measured radiation on cloudless days.

Date	Cloud cover 24 hours 10ths	Cloud cover daylight hours 10ths	Heat flux by incident shortwave radiation (Btu/sq ft day)	Heat flux by reflected shortwave radiation (Btu/sq ft day)	Heat flux by net all-wave radiation (Btu/sq ft day)	Heat flux by net longwave radiation (Btu/sq ft day)
4 Jan 66	0	0	+ 731	– 447	–349	–633
9 Jan 66	3	0	+ 782	– 569		
12 Jan 66	0	0	+ 789	– 409	–304	–684
22 Jan 66	2	0	+ 864	– 528		
29 Jan 66	3	0	+ 965	– 486		
7 Feb 66	0	0	+1147	– 581	– 24	–590
8 Feb 66	0	0	+1142	– 540	+ 83	–519
27 Feb 66	1	0	+1442	– 590		
15 Mar 66	2	0	+1778	– 716		
16 Mar 66	0	0	+1775	– 696	+283	–796
15 Apr 66	0	0	+2085	– 643	+864	–578
23 May 66	0	0	+2372	M*	M	M
16 Jul 66	0	0	+2473	M	M	M
21 Oct 66	0	0	+1154	– 424	+ 98	–632
27 Oct 66	0	0	+1090	– 405	+ 16	–669
13 Nov 66	0	0	+ 900	– 357	–142	–685
20 Nov 66	0	0	+ 794	– 338	–183	–639
21 Nov 66	0	0	+ 800	– 332	–169	–637
22 Nov 66	0	0	+ 751	– 315	–154	–590
4 Dec 66	0	0	+ 682	– 337	–209	–554
12 Dec 66	0	0	+ 643	– 277	–263	–629
19 Dec 66	1	0	+ 654	– 297		
6 Jan 67	0	0	+ 700	– 422	–235	–513
18 Jan 67	2	0	+ 816	– 382		
12 Feb 67	0	0	+1189	– 595	–114	–708
19 Mar 67	1	0	+1752	– 477		
25 Mar 67	0	0	+1792	– 644	+406	–742
						Avg –646

*M = Data missing.

APPENDIX C. HEAT FLUX FROM MEASURED TEMPERATURE GRADIENTS

Heat flux into/out of the ground was computed from gradients shown in Figures C1-C3. The procedure was: 1) Divide soil profile into layers determined when the slabs were installed. 2) Plot temperature gradients from measured temperatures and known sensor depths. 3) Obtain with a planimeter the area bounded by the limits of each layer and the temperature gradient. 4) Multiply area by a scale factor and volumetric specific heat to determine sensible heat loss. 5) Obtain latent heat by multiplying the change in thickness of the frozen layer by volumetric latent heat of layer. 6) Add results of items 4 and 5 to obtain heat loss from each layer. 7) Add losses from all layers to obtain heat loss for the desired time interval.

Measured temperatures were accurate within ±0.75°F and sensor spacing was accurate to 0.1 ft. Frost penetration depths were within ±0.2 ft. Using this information, measured heat fluxes were accurate to ±15%.

Soil properties for each material are:

Material	*Dry density (lb/cu ft)*	*Moisture content (%)*	*Volumetric specific heat (Btu/cu ft °F)*	*Volumetric latent heat (Btu/cu ft)*
Portland cement concrete	140	0	30	0
Sand	115	3.5	22.5	580
Silt 1	86	21.5	33	2660
Silt 2	86	32.5	42.5	4020

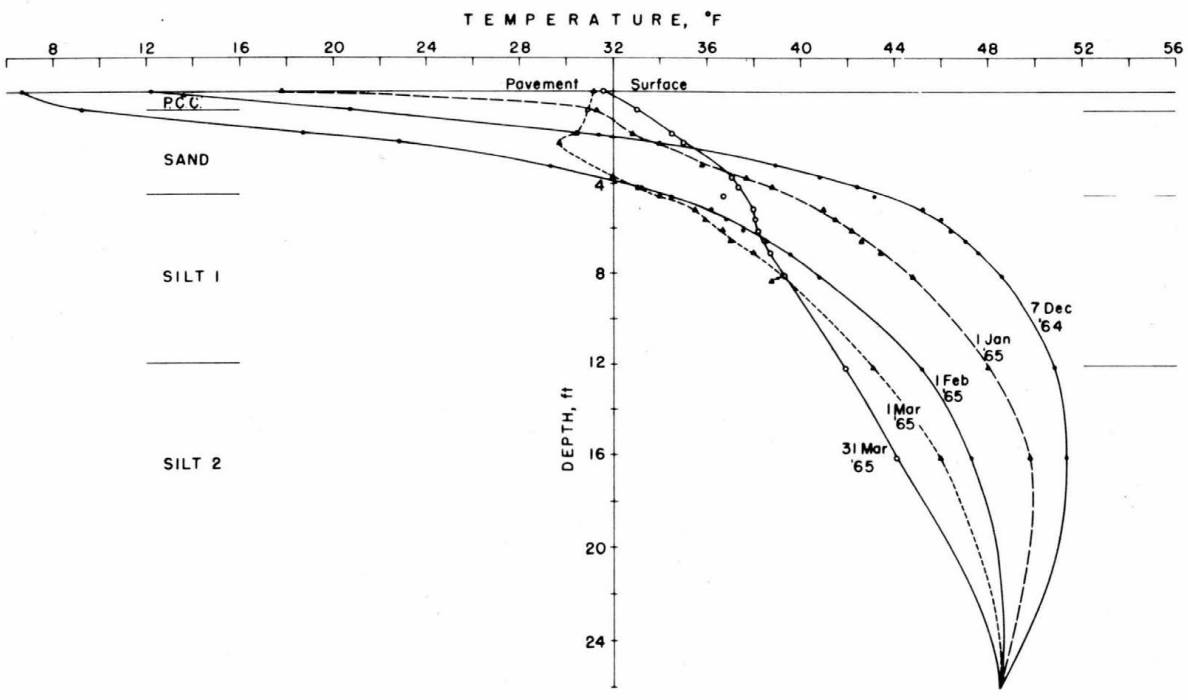

Figure C1. Temperature gradients, 1964-1965.

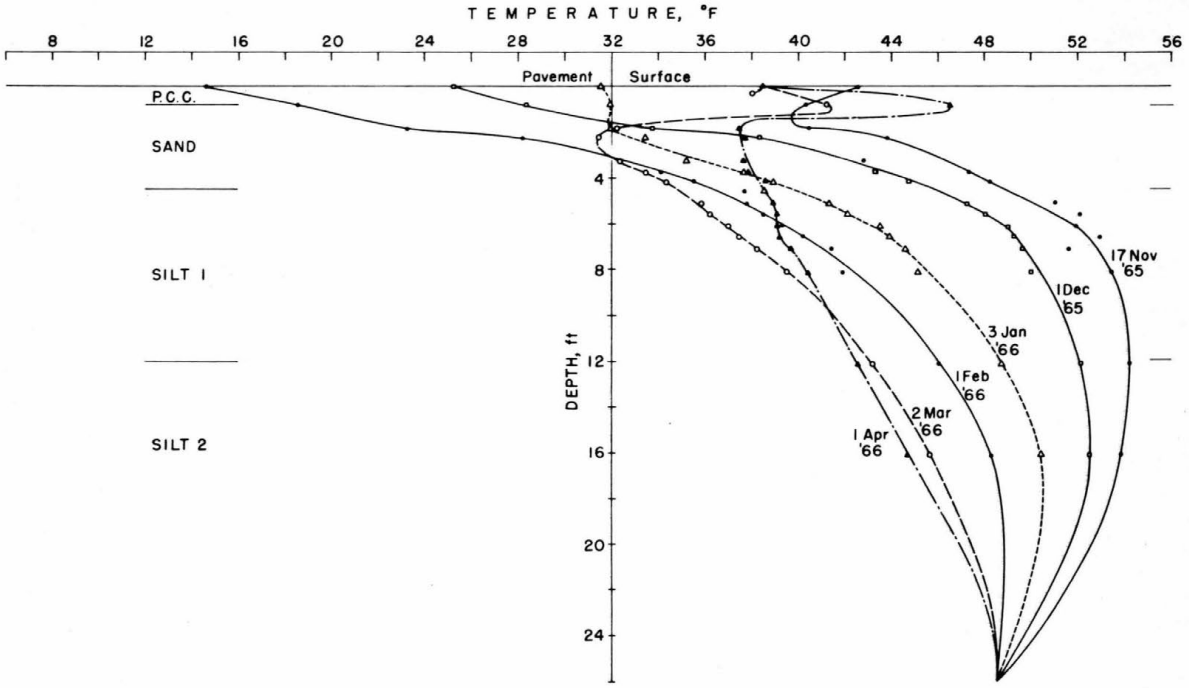

Figure C2. Temperature gradients, 1965-1966.

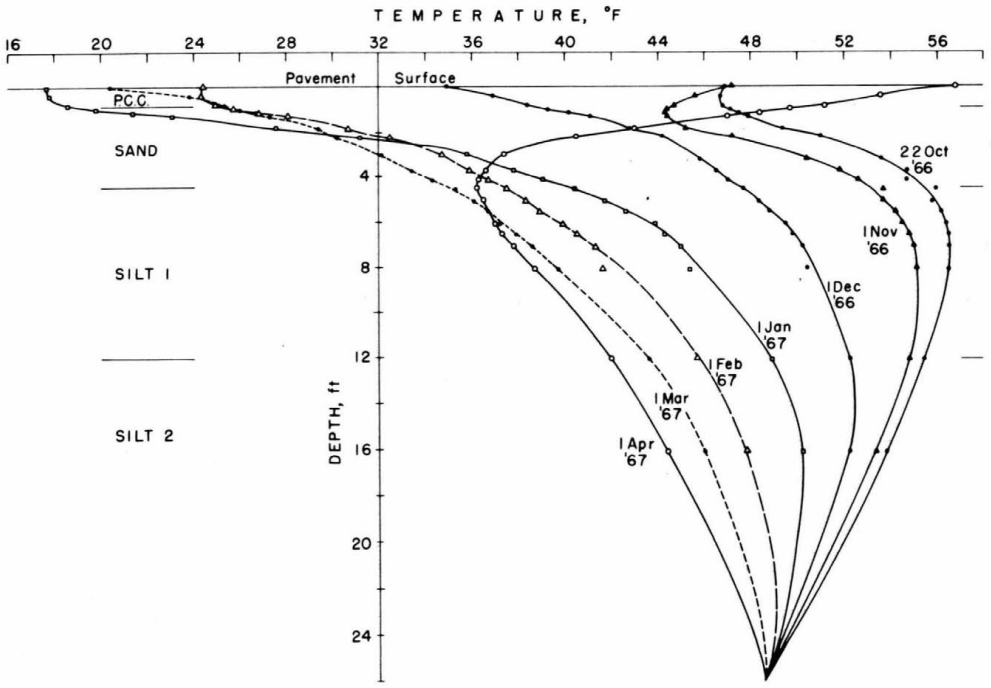

Figure C3. Temperature gradients, 1966-1967.

Heat fluxes are shown in Tables CI, CII and CIII for the 1964-1965, 1965-1966 and 1966-1967 winters, respectively.

Table CI. Heat flux, 1964-1965.

	Btu/sq ft			
Material	*7 Dec-1 Jan*	*1 Jan-1 Feb*	*1 Feb-1 Mar*	*1 Mar-31 Mar*
Portland cement concrete	+227	− 449	+562	+ 37
Sand	+402	−2309	+550	+2045
Silt 1	−945	− 963	−372	+ 86
Silt 2	−629	− 976	−498	− 656
Total	−945	−4697	+242	+1512

Table CII. Heat flux, 1965-1966.

	Btu/sq ft				
Material	*17 Nov-1 Dec*	*1 Dec-3 Jan*	*3 Jan-1 Feb*	*1 Feb-2 Mar*	*2 Mar-1 Apr*
Portland cement concrete	− 365	+ 125	− 385	+ 589	+ 97
Sand	− 879	− 547	−1212	+1226	+972
Silt 1	− 721	−1135	− 784	− 668	+234
Silt 2	− 624	− 855	− 925	− 976	−333
Total	−2589	−2412	−3306	+ 171	+970

Table CIII. Heat flux, 1966-1967.

	Btu/sq ft					
Material	*22 Oct-1 Nov*	*1 Nov-1 Dec*	*1 Dec-1 Jan*	*1 Jan-1 Feb*	*1 Feb-1 Mar*	*1 Mar-1 Apr*
Portland cement concrete	− 15	− 235	− 500	+ 175	− 30	+ 780
Sand	−280	− 330	−1875	+ 140	− 625	+2025
Silt 1	−330	−1085	−1205	− 840	− 640	− 215
Silt 2	−205	− 545	− 800	− 905	− 750	− 715
Total	−830	−2195	−4380	−1430	−2045	+1875

```
C     ENERGY BALANCE COMPUTER   R. BERG
C     WRITTEN 29 SEP 67, UPDT 15 JUL 68
C     ENERGY BALANCE COMPUTER   R. BERG
C     WRITTEN 29 SEP 67, UPDT 15 JUL 68
C     UPDT 6 AUG 68, LATEST UPDT 4 NOV 68.
      READ PAPER TAPE 1, LN
1     FORMAT(I4)
      QABSC=0.
      QNC=0.
      QAC=0.
      QCEC1=0.
      QGC1=0.
4     K=1
      PRINT 2
2     FORMAT(1H1,37X,32HENERGY BALANCE - LEBANON AIRPORT)
      PRINT 3
3     FORMAT(1HO,45X,17HCUMULATIVE FLUXES)
      PRINT 5
5     FORMAT(1HO,18X,2HSW,8X,2HLW,8X,3HNET,7X,3HC+S,8X,2HQG)
6     FORMAT(1H ,10X,3HDAY,5X,4HRAD.,6X,4HRAD.,6X,4HRAD.)
      PRINT 6
9     READ PAPER TAPE 7, N,CA,CD,U,TA,TS,JSUR
7     FORMAT(I4,5F8.3,I4)
C     CALCULATE ENERGY BALANCE COMPONENTS
      TS1=(459.7 + TS)/100.
      TA1=(459.7 + TA)/100.
      QN=2.85*(TA1**4-1.37*TS1**4)*(.992-.0785*CA)
22    IF(JSUR-1)23,24,25
23    ALB=.4
      GO TO 26
24    ALB=.5
      GO TO 26
25    ALB=.7
26    T=N
      IF(N-78)15,15,16
15    THETA=(283.+360.*T/365.)/57.29578
      GO TO 17
16    THETA=(360./365.)*(T-78.)/57.29578

17    A=SINF(THETA)
      QABS=(17.8+11.2*A)*(1.-ALB)*(96.-.71*CD**2)
      QC=4.1*U*(TA-TS)
30    QE=0.
33    QABSC=QABSC+QABS
      QNC=QNC+QN
      QAC=QAC+QABS+QN
      QCEC1=QCEC1+QC
      QGC1=QAC+QCEC1
      PRINT 8,N,QABSC,QNC,QAC,QCEC1,QGC1
8     FORMAT(1H ,10X,I3,5F10.0)
      K=K+1
      IF(N-LN)11,12,11
11    IF(K-34)9,4,10
10    PAUSE 1
      GO TO 4
12    STOP

      END
SUBROUTINES REQUIRED
   F$RT      F$TO      F$EL      F$T3      F$I       F$RS
   F$T1      F$WL      F$HD      F$X       F$F       F$FA
   F$FD      F$FM      F$C1      F$X2      F$FS      SINF
```

1964-1965

ENERGY BALANCE - LEBANON AIRPORT

CUMULATIVE FLUXES

DAY	SW RAD.	LW RAD.	NET RAD.	C+S	QG
342	181.	-228.	-47.	.	-47.
343	434.	-587.	-152.	-51.	-203.
344	775.	-1108.	-333.	-51.	-384.
345	875.	-1231.	-356.	-54.	-409.
346	999.	-1360.	-362.	-54.	-415.
347	1136.	-1494.	-358.	-34.	-392.
348	1473.	-1912.	-439.	12.	-427.
349	1765.	-2375.	-610.	-278.	-888.
350	2127.	-2726.	-600.	-243.	-842.
351	2278.	-2916.	-637.	-237.	-874.
352	2556.	-3326.	-770.	-406.	-1177.
353	2909.	-3764.	-855.	-452.	-1307.
354	2959.	-3883.	-925.	-454.	-1378.
355	3303.	-4246.	-943.	-474.	-1417.
356	3410.	-4417.	-1007.	-489.	-1496.
357	3510.	-4542.	-1032.	-443.	-1475.
358	3593.	-4659.	-1066.	-421.	-1487.
359	3694.	-4776.	-1082.	-224.	-1306.
360	3744.	-4887.	-1143.	-114.	-1257.
361	3795.	-5034.	-1239.	-217.	-1456.
362	3879.	-5190.	-1310.	-483.	-1793.
363	4271.	-5721.	-1450.	-558.	-2007.
364	4374.	-5855.	-1481.	-558.	-2038.
365	4578.	-6110.	-1532.	-674.	-2206.
1	4977.	-6717.	-1740.	-949.	-2689.
2	5029.	-6969.	-1940.	-993.	-2932.
3	5353.	-7313.	-1959.	-1102.	-3061.
4	5749.	-7840.	-2090.	-1214.	-3304.
5	6020.	-8206.	-2185.	-1214.	-3399.
6	6434.	-8679.	-2245.	-1211.	-3455.
7	6641.	-9153.	-2512.	-1211.	-3722.
8	6733.	-9267.	-2535.	-1204.	-3738.
9	6831.	-9426.	-2595.	-1029.	-3624.
10	6943.	-9606.	-2663.	-1049.	-3712.
11	7294.	-10015.	-2721.	-1056.	-3777.
12	7671.	-10415.	-2744.	-1066.	-3809.
13	7825.	-10633.	-2808.	-1060.	-3868.
14	8017.	-11150.	-3133.	-1479.	-4612.
15	8471.	-11703.	-3233.	-1557.	-4790.
16	8530.	-11893.	-3363.	-1591.	-4954.
17	8744.	-12265.	-3520.	-1665.	-5185.
18	9132.	-12546.	-3414.	-1665.	-5079.
19	9581.	-12871.	-3290.	-1653.	-4943.
20	9657.	-13024.	-3366.	-1482.	-4848.
21	10146.	-13431.	-3285.	-1430.	-4714.
22	10482.	-13699.	-3218.	-1297.	-4514.
23	10612.	-13820.	-3208.	-1363.	-4571.
24	10678.	-13936.	-3258.	-1372.	-4630.
25	11051.	-14215.	-3164.	-1332.	-4496.
26	11203.	-14414.	-3211.	-1353.	-4563.
27	11299.	-14627.	-3329.	-1243.	-4572.
28	11455.	-14967.	-3512.	-1350.	-4861.
29	11966.	-15527.	-3560.	-1751.	-5311.
30	12517.	-16066.	-3549.	-1824.	-5373.
31	13045.	-16475.	-3431.	-1820.	-5250.
32	13167.	-16701.	-3533.	-1826.	-5359.
33	13578.	-16965.	-3387.	-1779.	-5166.
34	14118.	-17458.	-3340.	-1880.	-5220.
35	14692.	-17952.	-3260.	-1937.	-5197.
36	14849.	-18223.	-3374.	-2025.	-5399.
37	14981.	-18316.	-3335.	-1987.	-5323.
38	15257.	-18461.	-3204.	-1865.	-5070.
39	15392.	-18587.	-3195.	-1794.	-4989.
40	16017.	-19241.	-3224.	-1963.	-5187.
41	16156.	-19389.	-3232.	-2043.	-5275.
42	16622.	-19737.	-3115.	-2029.	-5144.
43	16765.	-19897.	-3132.	-2055.	-5188.
44	17379.	-20430.	-3051.	-2312.	-5362.
45	17838.	-20857.	-3019.	-2353.	-5372.
46	18523.	-21428.	-2905.	-2353.	-5258.
47	19120.	-21932.	-2812.	-2406.	-5217.
48	19826.	-22624.	-2798.	-2466.	-5263.
49	19984.	-22868.	-2884.	-2692.	-5576.
50	20564.	-23213.	-2649.	-2697.	-5346.
51	21300.	-23861.	-2561.	-3011.	-5572.
52	21461.	-24001.	-2539.	-3011.	-5551.
53	21772.	-24372.	-2600.	-3249.	-5849.
54	22538.	-24991.	-2454.	-3471.	-5925.
55	23170.	-25463.	-2293.	-3577.	-5870.
56	23272.	-25583.	-2311.	-3551.	-5861.
57	23623.	-25862.	-2239.	-3577.	-5816.

1964-1965

ENERGY BALANCE - LEBANON AIRPORT

CUMULATIVE FLUXES

DAY	SW RAD.	LW RAD.	NET RAD.	C+S	QG
58	24421.	-26513.	-2092.	-3779.	-5871.
59	25132.	-27013.	-1881.	-4102.	-5983.
60	25587.	-27463.	-1876.	-4219.	-6096.
61	26426.	-28188.	-1763.	-4346.	-6108.
62	26842.	-28657.	-1815.	-4358.	-6173.
63	27676.	-29332.	-1655.	-4619.	-6274.
64	28114.	-29682.	-1568.	-4781.	-6349.
65	28327.	-29824.	-1497.	-4802.	-6299.
66	28572.	-29969.	-1397.	-4801.	-6198.
67	29415.	-30550.	-1135.	-4934.	-6070.
68	30167.	-31036.	-869.	-4978.	-5847.
69	30632.	-31379.	-747.	-5026.	-5774.
70	31565.	-32027.	-462.	-5491.	-5954.
71	32510.	-32716.	-205.	-5700.	-5906.
72	33417.	-33382.	35.	-5906.	-5871.
73	34177.	-33889.	288.	-6084.	-5796.
74	35108.	-34517.	591.	-6192.	-5601.
75	35750.	-34926.	824.	-6305.	-5480.
76	36609.	-35419.	1189.	-6500.	-5311.
77	36829.	-35570.	1259.	-6681.	-5423.
78	37408.	-35986.	1422.	-6998.	-5576.
79	37695.	-36321.	1373.	-7127.	-5754.
80	38363.	-36727.	1635.	-7416.	-5780.
81	39209.	-37150.	2059.	-7763.	-5705.
82	39349.	-37291.	2058.	-7813.	-5755.
83	40429.	-37993.	2436.	-8075.	-5639.
84	41495.	-38591.	2904.	-8272.	-5368.
85	41639.	-38739.	2900.	-8300.	-5460.
86	42663.	-39312.	3351.	-8983.	-5632.
87	43747.	-40050.	3697.	-9154.	-5456.
88	43895.	-40293.	3602.	-9183.	-5581.
89	44892.	-40797.	4095.	-9484.	-5389.
90	46050.	-41511.	4539.	-9822.	-5283.

1965-1966

ENERGY BALANCE - LEBANON AIRPORT

CUMULATIVE FLUXES

DAY	SW RAD.	LW RAD.	NET RAD.	C+S	QG
321	61.	-158.	-97.	-141.	-238.
322	163.	-531.	-368.	-525.	-893.
323	316.	-964.	-648.	-589.	-1237.
324	375.	-1245.	-870.	-594.	-1465.
325	433.	-1386.	-953.	-594.	-1547.
326	529.	-1546.	-1017.	-612.	-1629.
327	936.	-1759.	-823.	-808.	-1631.
328	1193.	-2202.	-1008.	-977.	-1985.
329	1530.	-2583.	-1053.	-1017.	-2070.
330	1653.	-2797.	-1144.	-1107.	-2251.
331	1707.	-3066.	-1359.	-1236.	-2594.
332	1998.	-3430.	-1432.	-1297.	-2728.
333	2179.	-3814.	-1635.	-1506.	-3141.
334	2457.	-4263.	-1806.	-1602.	-3408.
335	2741.	-4726.	-1985.	-1650.	-3635.
336	2846.	-4911.	-2065.	-1656.	-3721.
337	3170.	-5136.	-1966.	-1671.	-3637.
338	3285.	-5298.	-2013.	-1701.	-3714.
339	3493.	-5587.	-2094.	-1804.	-3897.
340	3545.	-5766.	-2222.	-2079.	-4301.
341	3931.	-6371.	-2440.	-2412.	-4852.
342	4107.	-6757.	-2650.	-2426.	-5076.
343	4481.	-7144.	-2663.	-2430.	-5092.
344	4811.	-7519.	-2708.	-2416.	-5124.
345	4986.	-7713.	-2727.	-2469.	-5196.
346	5036.	-7850.	-2815.	-2644.	-5459.
347	5085.	-7988.	-2903.	-2689.	-5592.
348	5185.	-8132.	-2947.	-2689.	-5636.
349	5267.	-8279.	-3012.	-2723.	-5735.
350	5430.	-8446.	-3016.	-2748.	-5763.
351	5625.	-8611.	-2986.	-2777.	-5762.
352	5778.	-8854.	-3076.	-2822.	-5898.
353	6034.	-9299.	-3265.	-2969.	-6234.
354	6414.	-9910.	-3496.	-3020.	-6516.
355	6759.	-10302.	-3543.	-3039.	-6581.
356	7120.	-10714.	-3594.	-2964.	-6558.
357	7263.	-10850.	-3586.	-2962.	-6548.
358	7387.	-11012.	-3625.	-2959.	-6584.
359	7472.	-11306.	-3834.	-2990.	-6824.
360	7646.	-11746.	-4100.	-3328.	-7428.

1965-1966

ENERGY BALANCE - LEBANON AIRPORT

CUMULATIVE FLUXES

DAY	SW RAD.	LW RAD.	NET RAD.	C+S	QG
361	7885.	-12111.	-4226.	-3369.	-7595.
362	8268.	-12487.	-4219.	-3363.	-7582.
363	8376.	-12705.	-4329.	-3350.	-7678.
364	8479.	-12830.	-4351.	-3347.	-7699.
365	8605.	-13001.	-4395.	-3310.	-7706.
1	8801.	-13297.	-4496.	-3345.	-7841.
2	8853.	-13533.	-4679.	-3441.	-8121.
3	8915.	-13679.	-4764.	-3505.	-8269.
4	9323.	-14300.	-4977.	-3568.	-8545.
5	9733.	-14805.	-5072.	-3568.	-8640.
6	9787.	-14939.	-5152.	-3580.	-8733.
7	9955.	-15162.	-5208.	-3625.	-8833.
8	10010.	-15327.	-5317.	-4044.	-9361.
9	10437.	-15905.	-5469.	-4354.	-9823.
10	10724.	-16192.	-5467.	-4379.	-9846.
11	11108.	-16582.	-5474.	-4620.	-10095.
12	11548.	-17177.	-5629.	-4773.	-10402.
13	11917.	-17530.	-5613.	-4780.	-10393.
14	12290.	-17888.	-5598.	-4826.	-10424.
15	12741.	-18362.	-5621.	-4893.	-10514.
16	13122.	-18881.	-5759.	-5089.	-10848.
17	13321.	-19105.	-5784.	-5167.	-10951.
18	13471.	-19380.	-5909.	-5184.	-11092.
19	13533.	-19521.	-5988.	-5186.	-11174.
20	13640.	-19788.	-6148.	-5192.	-11340.
21	13767.	-19979.	-6212.	-5207.	-11419.
22	14262.	-20519.	-6258.	-5212.	-11470.
23	14327.	-20649.	-6322.	-5345.	-11667.
24	14408.	-20850.	-6442.	-5536.	-11977.
25	14888.	-21376.	-6488.	-5676.	-12164.
26	15368.	-21852.	-6484.	-5676.	-12160.
27	15473.	-22040.	-6567.	-5753.	-12320.
28	16009.	-22661.	-6652.	-6323.	-12975.
29	16551.	-23120.	-6569.	-6367.	-12935.
30	16623.	-23230.	-6607.	-6234.	-12840.
31	16834.	-23482.	-6648.	-6416.	-13065.
32	17307.	-23919.	-6612.	-6484.	-13095.
33	17696.	-24171.	-6475.	-6486.	-12961.
34	18054.	-24346.	-6292.	-6486.	-12778.
35	18324.	-24532.	-6209.	-6487.	-12696.
36	18502.	-24906.	-6405.	-6646.	-13051.

1965-1966

ENERGY BALANCE - LEBANON AIRPORT

CUMULATIVE FLUXES

DAY	SW RAD.	LW RAD.	NET RAD.	C+S	QG
37	19102.	-25507.	-6404.	-6777.	-13181.
38	19717.	-26144.	-6427.	-6804.	-13231.
39	20341.	-26732.	-6392.	-6843.	-13235.
40	20551.	-26971.	-6420.	-6907.	-13327.
41	20959.	-27319.	-6360.	-7007.	-13366.
42	21371.	-27646.	-6275.	-6905.	-13180.
43	21837.	-28130.	-6293.	-7031.	-13324.
44	21924.	-28376.	-6452.	-7071.	-13524.
45	22179.	-28631.	-6452.	-7079.	-13531.
46	22419.	-29080.	-6661.	-7128.	-13789.
47	22509.	-29282.	-6773.	-7319.	-14092.
48	23148.	-29793.	-6645.	-7777.	-14422.
49	23431.	-30217.	-6786.	-8229.	-15015.
50	23614.	-30617.	-7003.	-8753.	-15756.
51	23936.	-31139.	-7204.	-9253.	-16457.
52	24610.	-31600.	-6991.	-9506.	-16496.
53	25051.	-31966.	-6915.	-9668.	-16583.
54	25808.	-32638.	-6830.	-9704.	-16533.
55	26468.	-33096.	-6629.	-9738.	-16366.
56	26570.	-33235.	-6665.	-9918.	-16583.
57	26836.	-33612.	-6776.	-10139.	-16915.
58	27643.	-34293.	-6650.	-10185.	-16835.
59	27850.	-34459.	-6609.	-10246.	-16855.
60	28070.	-34611.	-6542.	-10346.	-16887.
61	28753.	-35031.	-6278.	-10479.	-16756.
62	29593.	-35621.	-6028.	-10485.	-16513.
63	29841.	-35875.	-6034.	-10512.	-16546.
64	30030.	-36017.	-5987.	-10535.	-16521.
65	30183.	-36186.	-6003.	-10546.	-16549.
66	30948.	-36603.	-5655.	-10890.	-16545.
67	31844.	-37313.	-5469.	-11311.	-16780.
68	32705.	-37936.	-5231.	-11332.	-16563.
69	33564.	-38386.	-4821.	-11463.	-16285.
70	34497.	-39126.	-4629.	-11727.	-16356.
71	34699.	-39424.	-4725.	-11813.	-16538.
72	34824.	-39566.	-4742.	-11832.	-16575.
73	35755.	-40205.	-4450.	-12044.	-16493.
74	36735.	-40900.	-4165.	-12556.	-16721.
75	37726.	-41670.	-3944.	-12719.	-16663.
76	38657.	-42186.	-3529.	-12797.	-16326.
77	39620.	-42480.	-2860.	-12625.	-15485.

1965-1966

ENERGY BALANCE - LEBANON AIRPORT

CUMULATIVE FLUXES

DAY	SW RAD.	LW RAD.	NET RAD.	C+S	QG
78	39962.	-42835.	-2873.	-12682.	-15554.
79	40417.	-43152.	-2735.	-12722.	-15457.
80	41353.	-43666.	-2314.	-12792.	-15105.
81	41775.	-44128.	-2354.	-12968.	-15321.
82	42007.	-44280.	-2273.	-13031.	-15304.
83	42241.	-44419.	-2177.	-13042.	-15219.
84	42867.	-44769.	-1902.	-13394.	-15296.
85	43625.	-45113.	-1488.	-13566.	-15053.
86	44422.	-45540.	-1118.	-14056.	-15174.
87	45079.	-45990.	-911.	-14406.	-15317.
88	45930.	-46568.	-639.	-14630.	-15269.
89	46179.	-46796.	-617.	-14734.	-15351.
90	46855.	-47196.	-341.	-15019.	-15360.

1966-1967

ENERGY BALANCE - LEBANON AIRPORT

CUMULATIVE FLUXES

DAY	SW RAD.	LW RAD.	NET RAD.	C+S	QG
295	601.	-441.	160.	-2.	157.
296	998.	-835.	163.	7.	169.
297	1551.	-1324.	227.	6.	233.
298	2183.	-1881.	302.	-5.	297.
299	2800.	-2577.	223.	-5.	218.
300	3420.	-3258.	162.	-7.	154.
301	4027.	-3894.	132.	-1.	131.
302	4447.	-4319.	128.	30.	158.
303	5004.	-4921.	83.	-157.	-73.
304	5284.	-5194.	91.	-209.	-118.
305	5641.	-5454.	186.	-175.	11.
306	5906.	-5620.	286.	-179.	107.
307	6169.	-5932.	238.	-288.	-50.
308	6665.	-6541.	124.	-393.	-269.
309	7019.	-6868.	151.	-411.	-259.
310	7136.	-7011.	125.	-422.	-296.
311	7380.	-7224.	157.	-426.	-269.
312	7517.	-7359.	158.	-411.	-253.
313	7652.	-7497.	156.	-387.	-232.
314	7763.	-7653.	110.	-327.	-217.
315	7985.	-7898.	87.	-365.	-279.
316	8115.	-8133.	-19.	-394.	-413.
317	8606.	-8884.	-277.	-535.	-812.
318	9006.	-9306.	-300.	-556.	-856.
319	9264.	-9713.	-449.	-706.	-1155.
320	9388.	-9959.	-571.	-730.	-1301.
321	9579.	-10116.	-537.	-717.	-1254.
322	9680.	-10247.	-567.	-676.	-1244.
323	10107.	-10715.	-608.	-753.	-1361.
324	10559.	-11331.	-771.	-759.	-1531.
325	11007.	-11904.	-898.	-757.	-1655.
326	11449.	-12441.	-992.	-757.	-1749.
327	11863.	-12876.	-1012.	-757.	-1769.
328	12071.	-13164.	-1094.	-757.	-1851.
329	12179.	-13310.	-1130.	-736.	-1866.
330	12437.	-13551.	-1114.	-736.	-1849.
331	12546.	-13713.	-1167.	-736.	-1902.
332	12661.	-13865.	-1204.	-707.	-1911.
333	12901.	-14179.	-1278.	-737.	-2015.
334	12990.	-14382.	-1392.	-751.	-2143.
335	13159.	-14533.	-1374.	-728.	-2102.

1966-1967

ENERGY BALANCE - LEBANON AIRPORT

CUMULATIVE FLUXES

DAY	SW RAD.	LW RAD.	NET RAD.	C+S	QG
336	13329.	-14895.	-1566.	-757.	-2324.
337	13691.	-15418.	-1726.	-784.	-2510.
338	14090.	-15962.	-1872.	-789.	-2662.
339	14438.	-16298.	-1860.	-789.	-2649.
340	14689.	-16496.	-1807.	-775.	-2582.
341	14774.	-16637.	-1863.	-775.	-2638.
342	14859.	-16757.	-1899.	-762.	-2661.
343	15063.	-16915.	-1853.	-747.	-2599.
344	15163.	-17035.	-1872.	-662.	-2534.
345	15269.	-17325.	-2056.	-691.	-2747.
346	15652.	-17963.	-2311.	-768.	-3080.
347	15805.	-18258.	-2453.	-768.	-3221.
348	15855.	-18398.	-2543.	-796.	-3339.
349	16191.	-18888.	-2697.	-912.	-3609.
350	16417.	-19212.	-2795.	-952.	-3747.
351	16580.	-19478.	-2899.	-937.	-3836.
352	16684.	-19641.	-2956.	-891.	-3848.
353	17065.	-20195.	-3131.	-960.	-4091.
354	17315.	-20473.	-3158.	-982.	-4140.
355	17431.	-20663.	-3232.	-992.	-4225.
356	17584.	-20834.	-3250.	-1008.	-4258.
357	17922.	-21256.	-3335.	-973.	-4308.
358	18044.	-21500.	-3456.	-972.	-4428.
359	18121.	-21712.	-3591.	-1086.	-4678.
360	18334.	-22138.	-3805.	-1218.	-5023.
361	18696.	-22574.	-3878.	-1218.	-5096.
362	19061.	-22922.	-3862.	-1218.	-5080.
363	19139.	-23109.	-3970.	-1181.	-5151.
364	19506.	-23531.	-4026.	-1288.	-5313.
365	19876.	-23950.	-4074.	-1301.	-5375.
1	19928.	-24110.	-4182.	-1301.	-5484.
2	20256.	-24452.	-4196.	-1293.	-5489.
3	20402.	-24578.	-4176.	-1293.	-5469.
4	20455.	-24694.	-4239.	-1293.	-5532.
5	20512.	-24854.	-4343.	-1291.	-5634.
6	20927.	-25491.	-4565.	-1360.	-5924.
7	21010.	-25753.	-4742.	-1360.	-6102.
8	21133.	-25859.	-4727.	-1360.	-6086.
9	21474.	-26239.	-4765.	-1382.	-6147.
10	21721.	-26483.	-4762.	-1382.	-6144.
11	22048.	-26873.	-4825.	-1393.	-6217.
12	22105.	-27052.	-4947.	-1426.	-6373.
13	22345.	-27300.	-4955.	-1425.	-6380.
14	22442.	-27477.	-5034.	-1425.	-6459.
15	22727.	-27764.	-5037.	-1444.	-6481.
16	23175.	-28337.	-5162.	-1509.	-6671.
17	23504.	-28555.	-5052.	-1456.	-6507.
18	23974.	-29102.	-5128.	-1599.	-6726.
19	24363.	-29536.	-5173.	-1634.	-6807.
20	24811.	-29934.	-5123.	-1634.	-6757.
21	25226.	-30231.	-5004.	-1601.	-6606.
22	25526.	-30490.	-4964.	-1588.	-6552.
23	25635.	-30671.	-5036.	-1583.	-6620.
24	26083.	-31050.	-4967.	-1566.	-6533.
25	26217.	-31184.	-4968.	-1578.	-6545.
26	26497.	-31371.	-4873.	-1600.	-6473.
27	26612.	-31511.	-4898.	-1653.	-6551.
28	26686.	-31662.	-4976.	-1678.	-6655.
29	26881.	-31889.	-5008.	-1809.	-6817.
30	27376.	-32340.	-4964.	-1872.	-6836.
31	27645.	-32783.	-5138.	-1872.	-7010.
32	27768.	-32902.	-5134.	-1872.	-7006.
33	27842.	-33031.	-5189.	-1892.	-7081.
34	28420.	-33747.	-5326.	-2148.	-7474.
35	28497.	-33965.	-5468.	-2183.	-7651.
36	29084.	-34236.	-5153.	-2094.	-7247.
37	29644.	-34831.	-5187.	-2508.	-7696.
38	29724.	-35121.	-5397.	-2610.	-8007.
39	30334.	-35708.	-5374.	-2679.	-8053.
40	30961.	-36152.	-5192.	-2683.	-7874.
41	31442.	-36456.	-5014.	-2706.	-7721.
42	31764.	-36739.	-4974.	-2723.	-7697.
43	32424.	-37359.	-4935.	-2930.	-7865.
44	33085.	-37946.	-4861.	-2930.	-7791.
45	33467.	-38299.	-4832.	-2955.	-7787.
46	33905.	-38566.	-4660.	-2939.	-7600.
47	34218.	-38922.	-4704.	-3175.	-7880.
48	34867.	-39516.	-4649.	-3275.	-7923.
49	35218.	-39910.	-4692.	-3275.	-7966.
50	35905.	-40469.	-4564.	-3275.	-7839.
51	36000.	-40630.	-4630.	-3275.	-7904.
52	36097.	-40838.	-4740.	-3304.	-8044.

1966-1967

ENERGY BALANCE - LEBANON AIRPORT

CUMULATIVE FLUXES

DAY	SW RAD.	LW RAD.	NET RAD.	C+S	QG
53	36809.	-41303.	-4494.	-3386.	-7880.
54	36909.	-41440.	-4532.	-3454.	-7985.
55	37597.	-41915.	-4318.	-3804.	-8122.
56	37809.	-42294.	-4485.	-4124.	-8609.
57	38599.	-42860.	-4260.	-4307.	-8568.
58	39177.	-43241.	-4064.	-4457.	-8521.
59	39301.	-43428.	-4127.	-4551.	-8677.
60	40084.	-44062.	-3978.	-4944.	-8922.
61	40432.	-44355.	-3923.	-5034.	-8957.
62	40678.	-44579.	-3901.	-5034.	-8936.
63	41355.	-45189.	-3834.	-5353.	-9186.
64	41481.	-45404.	-3923.	-5430.	-9352.
65	41603.	-45535.	-3932.	-5430.	-9362.
66	41966.	-45848.	-3881.	-5514.	-9395.
67	42561.	-46381.	-3820.	-5578.	-9398.
68	43143.	-46831.	-3688.	-5607.	-9295.
69	44011.	-47308.	-3297.	-5637.	-8934.
70	44760.	-47642.	-2883.	-5638.	-8521.
71	45695.	-48331.	-2636.	-5892.	-8528.
72	46079.	-48610.	-2531.	-6103.	-8634.
73	46313.	-48811.	-2498.	-6131.	-8629.
74	46440.	-48994.	-2554.	-6150.	-8704.
75	46829.	-49492.	-2663.	-6926.	-9589.
76	47760.	-50136.	-2376.	-7180.	-9556.
77	48741.	-50809.	-2069.	-7388.	-9456.
78	49765.	-51504.	-1739.	-7511.	-9250.
79	50732.	-52147.	-1415.	-7633.	-9048.
80	51152.	-52445.	-1293.	-7724.	-9017.
81	51443.	-52663.	-1220.	-7750.	-8970.
82	51955.	-52987.	-1032.	-7782.	-8814.
83	52964.	-53451.	-487.	-7886.	-8373.
84	54055.	-54175.	-120.	-8004.	-8124.
85	55150.	-54931.	220.	-8031.	-7811.
86	55885.	-55418.	468.	-8102.	-7634.
87	56228.	-55577.	650.	-8111.	-7461.
88	56962.	-55955.	1008.	-8159.	-7151.
89	58108.	-56611.	1497.	-8218.	-6720.
90	59161.	-57217.	1944.	-8269.	-6326.

DOCUMENT CONTROL DATA - R & D

(Security classification of title, body of abstract and indexing annotation must be entered when the overall report is classified)

1. ORIGINATING ACTIVITY *(Corporate author)*
U. S. Army Cold Regions Research and Engineering Laboratory
Hanover, New Hampshire 03755

2a. REPORT SECURITY CLASSIFICATION
Unclassified

2b. GROUP

3. REPORT TITLE
ENERGY BALANCE ON A PAVED SURFACE

4. DESCRIPTIVE NOTES *(Type of report and inclusive dates)*

5. AUTHOR(S) *(First name, middle initial, last name)*
Richard L. Berg

6. REPORT DATE
June 1974

7a. TOTAL NO. OF PAGES
56

7b. NO. OF REFS
41

8a. CONTRACT OR GRANT NO.

b. PROJECT NO.

c. Sub-project 42

d.

9a. ORIGINATOR'S REPORT NUMBER(S)
Technical Report 226

9b. OTHER REPORT NO(S) *(Any other numbers that may be assigned this report)*

10. DISTRIBUTION STATEMENT
Approved for public release; distribution unlimited.

11. SUPPLEMENTARY NOTES

12. SPONSORING MILITARY ACTIVITY
Directorate of Military Construction
Office, Chief of Engineers
Washington, D.C.

13. ABSTRACT

Energy balance data from portland cement concrete test slabs at the Lebanon Regional Airport, Lebanon, New Hampshire, are compared with calculated quantities. Energy balance components are calculated from techniques used by Scott in developing the cumulative heat flow technique for determining frost and thaw depths. Techniques for computing frost and thaw depths are briefly reviewed to illustrate applications of the surface energy balance in frost and thaw depth calculations. Comparison of calculated and measured components of the energy balance indicates that computational techniques and/or data measurement techniques must be improved to provide estimated frost and thaw depths that are within 15% of measured depths.

14. Key Words:
Concrete pavements
Energy balance
Frost and thaw penetration
Heat transfer

DD FORM 1 NOV 1473 REPLACES DD FORM 1473, 1 JAN 64, WHICH IS OBSOLETE FOR ARMY USE.